Descriptive anatomy of the largest known specimen of *Protoichthyosaurus prostaxalis* (Reptilia: Ichthyosauria) including computed tomography and digital reconstruction of a three-dimensional skull

Dean R. Lomax [Corresp., 1] , **Laura B. Porro** [2] , **Nigel R. Larkin** [3]

[1] School of Earth and Environmental Sciences, University of Manchester, Manchester, United Kingdom

[2] Department of Cell and Developmental Biology, University College London, London, United Kingdom

[3] Cambridge University Museum of Zoology, Cambridge, United Kingdom

Corresponding Author: Dean R. Lomax
Email address: dean.lomax@manchester.ac.uk

Ichthyosaur fossils are abundant in Lower Jurassic sediments with nine genera found in the UK. In this paper, we describe the partial skeleton of a large ichthyosaur from the Lower Jurassic (lower Sinemurian) of Warwickshire, England, which was conserved and rearticulated to form the centerpiece of a new permanent gallery at the Thinktank, Birmingham Science Museum in 2015. The unusual three-dimensional preservation of the specimen permitted computed tomography scanning of individual braincase elements as well as the entire reassembled skull. This represents one of the first times that medical imaging and three-dimensional reconstruction methods have been applied to a large skull of a marine reptile. Data from these scans provide new anatomical information, such as the presence of branching vascular canals within the premaxilla and dentary, and an undescribed dorsal (quadrate) wing of the pterygoid hidden within matrix. Scanning also revealed areas of the skull that had been modelled in wood, clay and other materials after the specimen's initial discovery, highlighting the utility of applying advanced imaging techniques to historical specimens. Additionally, the CT data served as the basis for a new three-dimensional reconstruction of the skull, in which minor damage was repaired and the preserved bones digitally rearticulated. Thus, for the first time a digital reconstruction of the skull and mandible of a large marine reptile skull is available. Museum records show the specimen was originally identified as an example of *Ichthyosaurus communis* but we identify this specimen as *Protoichthyosaurus prostaxalis*. The specimen features a skull nearly twice as long as any previously described specimen of *P. prostaxalis,* representing an individual with an estimated total body length between 3.2 and 4 meters.

1   **Descriptive anatomy of the largest known specimen of *Protoichthyosaurus prostaxalis***

2   **(Reptilia: Ichthyosauria) including computed tomography and digital reconstruction of a**

3   **three-dimensional skull**

5   **Dean R. Lomax[1], Laura B. Porro[2], Nigel R. Larkin[3]**

6   [1] School of Earth and Environmental Sciences, The University of Manchester, Oxford Rd,

7   Manchester, M13 9PL, United Kingdom

8   [2] Department of Cell and Developmental Biology, University College London, WC1E 6BT,

9   United Kingdom

10   [3] Cambridge University Museum of Zoology, Downing St, Cambridge, CB2 3EJ, United

11   Kingdom

13   Corresponding Author: Dean R. Lomax, dean.lomax@manchester.ac.uk

Abstract

16   Ichthyosaur fossils are abundant in Lower Jurassic sediments with nine genera found in the UK.

17   In this paper, we describe the partial skeleton of a large ichthyosaur from the Lower Jurassic

18   (lower Sinemurian) of Warwickshire, England, which was conserved and rearticulated to form

19   the centerpiece of a new permanent gallery at the Thinktank, Birmingham Science Museum in

20   2015. The unusual three-dimensional preservation of the specimen permitted computed

21   tomography scanning of individual braincase elements as well as the entire reassembled skull.

22   This represents one of the first times that medical imaging and three-dimensional reconstruction

23   methods have been applied to a large skull of a marine reptile. Data from these scans provide

24   new anatomical information, such as the presence of branching vascular canals within the

25   premaxilla and dentary, and an undescribed dorsal (quadrate) wing of the pterygoid hidden

26   within matrix. Scanning also revealed areas of the skull that had been modelled in wood, clay

27   and other materials after the specimen's initial discovery, highlighting the utility of applying

28   advanced imaging techniques to historical specimens. Additionally, the CT data served as the

29   basis for a new three-dimensional reconstruction of the skull, in which minor damage was

30   repaired and the preserved bones digitally rearticulated. Thus, for the first time a digital

31   reconstruction of the skull and mandible of a large marine reptile skull is available. Museum

32   records show the specimen was originally identified as an example of *Ichthyosaurus communis*

33   but we identify this specimen as *Protoichthyosaurus prostaxalis*. The specimen features a skull

34   nearly twice as long as any previously described specimen of *P. prostaxalis,* representing an

35   individual with an estimated total body length between 3.2 and 4 meters.

37   **Introduction**

38   Ichthyosaurs were a highly successful group of predatory marine reptiles that appeared in the late

39   Early Triassic and went extinct in the early Late Cretaceous (Fischer et al., 2016). Some of the

40   earliest forms were 'lizard-like' in appearance, although later forms evolved fish-shaped bodies

41   (Motani, 2009). Species ranged in size from small-bodied forms less than 1 m long to giants over

42   20 m in length (Motani, 2005; Nicholls & Manabe, 2004; Lomax et al., 2018). Numerous Lower

43   Jurassic ichthyosaurs have been found in the UK, the majority being from the Lyme Regis-

44   Charmouth area in west Dorset (Milner & Walsh, 2010), the village of Street and surrounding

45   areas in Somerset (Delair, 1969), sites around the coastal town of Whitby, Yorkshire (Benton &

46   Taylor, 1984) and Barrow-upon-Soar, Leicestershire (Martin et al., 1986). Notable specimens

47   have also been recorded from Ilminster, Somerset (Williams et al., 2015), Nottinghamshire

48   (Lomax & Gibson, 2015) and Warwickshire (Smith & Radley, 2007), with various isolated

49   occurrences at other sites across the UK (Benton & Spencer, 1995).

50   A partial ichthyosaur skeleton (BMT 1955.G35.1 – Birmingham Museums Trust) was

51   discovered in 1955 in Warwickshire, England. The specimen comprises a largely complete skull,

52   portions of the pectoral girdle, pelvis, fore- and hindfins, and numerous vertebrae and ribs. Bones

53   of the basicranium and palate were also found, which are rarely observed in association with

54   Lower Jurassic ichthyosaur skulls (Marek et al., 2015). The skull bones were reassembled three-

55   dimensionally on a wood and metal frame held together with alvar, jute and kaolin dough, with

56   missing parts carved from wood; however, some aspects were not accurately reconstructed.

57   Museum records indicate that BMT 1955.G35.1, which has never been formally described, was

58   originally identified as an example of *Ichthyosaurus communis* De la Beche & Conybeare 1821.

59   In 2015, as part of the development of the new Marine Worlds Gallery at the Thinktank,

60   Birmingham Science Museum, the skull was dismantled, conserved and reassembled to be more

61   anatomically accurate. The skull and postcranial skeleton of BMT 1955.G35.1 were publicly

62   displayed for the first time, forming the centerpiece of this permanent gallery. The skull of BMT

63   1955.G35.1 is preserved in 3D and is free of matrix; this contrasts with the majority of Lower

64   Jurassic ichthyosaur skulls, which are often flattened or displaced and preserved in matrix,

65   enabling a more detailed description than is typical. The large size of many marine reptile skulls

66   has precluded attempts to visualize specimens using medical imaging (but see McGowan, 1989).

67   Given the exceptional 3D preservation, the fact it is relatively free of matrix, and access to

68   facilities capable of imaging large specimens, we took the opportunity to scan individual cranial

69   elements as well as the entire skull of BMT 1955.G35.1 using computed tomography (CT)

70   before and after reassembly. Computed tomography and 3D digital reconstruction are

71   increasingly being applied to the skulls of fossil vertebrates, including early tetrapods (Porro et

72   al., 2015*a,b*), dinosaurs (Rayfield et al., 2001; Lautenschlager et al., 2014, 2016; Porro et al.,

73   2015c; Button et al., 2016) and extinct synapsids (Wroe, 2007; Jasinoski et al., 2009; Sharp,

74   2014; Cox et al., 2015; Lautenschlager et al., 2017). The first attempt to understand the internal

75   anatomy of the ichthyosaur skull was carried out by Sollas (1916) using serial grinding; although

76   this method produced excellent understanding of skull anatomy, it was time-consuming, labour

77   intensive and resulted in the destruction of the specimen. In contrast, modern medical imaging

78   methods have been applied only to isolated regions of fossil marine reptile skulls (Kear, 2005;

79   Fernández et al., 2011; Sato et al., 2011; Neenan and Scheyer, 2012; Herrera et al., 2013), with

80   the exception of one pliosaur (Foffa et al., 2014a), one small ichthyosaur (Marek et al., 2015), for

81   which entire skulls were CT scanned, and the skeleton of a juvenile plesiosaur (Larkin et al.,

82   2010).

83   In this paper, we use CT scanning of a large ichthyosaur skull along with careful

84   examination of the original specimen to formally describe BMT 1955.G35.1. Based on this

85   description we reassign the specimen to *Protoichthyosaurus prostaxalis* Appleby 1979, a genus

86   recently shown to be distinct from *Ichthyosaurus* based on multiple characters (Lomax, Massare

87   & Mistry, 2017; Lomax & Massare, 2018). Furthermore, the studied specimen has an estimated

88   maximum body length of 3.2 to 4 metres, greater than any other known specimen of

89   *Protoichthyosaurus* or *Ichthyosaurus*.

90

91   **Geological setting**

92 BMT 1955.G35.1 was collected in situ from Fell Mill Farm, between Shipston-on-Stour and

93 Honington, Warwickshire, England, grid reference NGR SP 277 415. The initial discovery was

94 made by Mr Michael Bryan in May, 1955. A complete excavation, under the supervision of

95 Assistant Keeper of Natural History at the City of Birmingham Museum, Mr Vincent Smith,

96 subsequently took place. The specimen was found approximately 4 feet below the ground surface

97 in a hard, blue-grey clay, lying directly on top of a brown grit layer containing numerous

98 *Gryphaea* bivalves. Due to the fragmentary nature of the bones, they were removed embedded in

99 clay.

100   Precise stratigraphic data associated with the discovery are not available but the remains

101 were recorded as being from Liassic sediments, which conforms to the Early Jurassic age of the

102 region's geology (Edmonds et al., 1965; Radley, 2003; Smith & Radley, 2007). In addition to the

103 ichthyosaur skeleton, other fossils were collected alongside the specimen, including *Gryphaea*

104 bivalves, a plesiosaur vertebra, and an isolated shark tooth identified as *Hybodus* cf. *H. cloacinus*

105 Quenstedt 1858, which are also Early Jurassic in age, although this shark species ranges from the

106 Rhaetic through Lower Lias (N. R. Larkin, pers. comm. D. Ward, 2015). Additionally, we found

107 an ammonite fragment stored with the specimen, which is an example of *Euagassiceras*

108 *sauzeanum* (d'Orbigny 1844), a species indicative of the *Semicostatum* Ammonite Zone, lower

109 Sinemurian, Lower Jurassic (DRL pers. comm. M. Howarth, 2017). As there was no record

110 stating whether this ammonite fragment was physically collected with BMT 1955.G35.1, NRL

111 was given permission by the current owners of Fell Mill Farm to collect other fossils along with

112 matrix from the original site at a depth of 2 m below the surface. This resulted in the collection

113 of numerous ammonites identified as *Arnioceras semicostatum* (Young & Bird 1828), which is

114 also indicative of the lower Sinemurian, *Semicostatum* Ammonite Zone (DRL pers. comm. M.

115   Howarth, 2017). Thus, associated ammonites have provided the stratigraphic position of BMT

116   1955.G35.1.

117

118   **Material and methods**

119   BMT 1955.G35.1 is currently housed in the Thinktank Science Museum (TSM). It was originally

120   accessioned into the collections of Birmingham Museum and Art Gallery (BMAG) and loaned to

121   TSM. However, BMAG and TSM have since become part of the Birmingham Museums Trust

122   (BMT). The postcranial skeleton, long considered 'missing', was rediscovered in the collections

123   of the Lapworth Museum of Geology (BU) and reunited with the skull as part of a funded project

124   at the TSM. As BMT 1955.G35.1 was largely undeformed, the individual skull bones were

125   assembled in 3D; however, several errors were made in this original reconstruction (Fig. 1A). As

126   part of the funded project, the skull was disassembled and the individual bones cleaned,

127   conserved, and remounted (Fig. 1B-C). Many of the preserved skull bones were disarticulated

128   when discovered and several cranial bones are not represented. The teeth have been reset and are

129   not in their original positions. Portions of some elements are poorly preserved and/or

130   taphonomically distorted, which somewhat restricts our description; for example, the dentaries

131   cannot be articulated at the symphysis or mounted in their correct anatomical position. The

132   newly reassembled skull of BMT 1955.G35.1 is based on all the preserved elements robust

133   enough to safely include, and we limit our description of sutural contacts to those between

134   elements preserved in original articulation. Specific details of the reconstruction and

135   conservation of the studied specimen will be dealt with in a separate paper.

136   Prior to remounting, several individual bones of the left side of the skull were scanned

137   using microcomputed tomography (μCT) in March 2015 at the Cambridge Biotomography

138 Centre (Zoology Department, University of Cambridge) on an X-Tek H 225 μCT scanner (Nikon

139 Metrology, Tring, UK) at 135kV and 227 μA with no filtering. Elements scanned individually

140 include: the left articular, opisthotic, stapes, quadrate and pterygoid; the median supraoccipital

141 and basisphenoid; and both parietals. Voltage, current and resolution (0.1 mm/voxel) were

142 identical for all scans. Scan data were visualized in the software Avizo 8.0 (Thermo Fisher

143 Scientific, Waltham, Massachusetts, USA) and the left-side elements mirrored across the sagittal

144 midline. All 3D surfaces were exported as stereolithography (STL) files and 3D printed at life-

145 size in gypsum on a 3DS x60 3D Printer; pieces were subsequently dipped in cyanoacrylate for

146 strength (NRL pers. comm. S. Dey, 2016).

147 After remounting, the skull of BMT 1955.G35.1, including the 3D printouts previously

148 described, was scanned in May 2015 at the Royal Veterinary College on a Lightspeed Pro 16 CT

149 scanner (GE Medical Systems LTd., Pollards Wood, UK) at 120 kV and 200 μA. Due to the size

150 of the specimen, it was scanned in two parts – the front of the skull was scanned at

151 0.56x0.56x1.25 mm/voxel and the rear of the skull was scanned at 0.73x0.73x1.25 mm/voxel.

152 Both scans produced a total of 2168 DICOM slices. Both scans used an exposure time of 2356

153 ms and a body filter. Density thresholding was used to separate higher-density fossil bone from

154 lower-density matrix as well as areas of the skull historically modelled in wood, clay and jute,

155 and portions newly modelled in gypsum. Scans were segmented to isolate individual bones and

156 teeth, and to trace internal features. The two halves of the skull were overlain and merged using

157 skeletal landmarks visible in both datasets (Figs. 2-4). Three-dimensional surfaces were exported

158 as wavefront (OBJ) files to create an interactive 3D PDF using Tetra4D Reviewer and Converter

159 (Tech Soft 3D; Oregon, USA) and Adobe Acrobat Pro X (Adobe Systems, California, USA).

160 This reconstruction is provided as supporting information (Appendix S1) and are the basis for the

161 following description.

162   Surface models of individual bones were manipulated in 3D space using the Transform

163 Editor within Avizo, allowing digital 3D reconstruction of the skull of BMT 1955.G35.1

164 following similar methods applied to early tetrapods (Porro et al. 2015*a,b*) and dinosaurs

165 (Lautenschlager, 2016). Most of the bones in the digital reconstruction are from the left side of

166 BMT 1955.G35.1 as this side is generally better preserved. Minor damage was manually repaired

167 in the Segmentation Editor within Avizo using interpolation, including: minor breaks and

168 missing alveolar margins in the left premaxilla, maxilla, dentary and splenial; minor breaks in the

169 left nasal, lacrimal, jugal, quadrate, pterygoid, and parietal; the missing right margin of the

170 supraoccipital; and gaps within the anterior half of the left surangular. Portions of bones

171 preserved on the right but absent on the left – including the posterior tip of the right jugal and

172 anterior tip of the right splenial – were duplicated, reflected across the sagittal midline, and

173 merged with left side elements using anatomical landmarks. We did not attempt to reconstruct

174 missing bones or preserved elements that could not be scanned due to their delicate nature (see

175 Results). The disarticulated bones were then fitted together at sutural contacts; we also referred

176 to known relationships between skull bones from other ichthyosaur skulls (Andrews, 1910;

177 Sollas, 1916; McGowan, 1973; Kirton, 1983; McGowan & Motani, 2003; Marek et al., 2015;

178 Moon & Kirton, 2016). Lastly, left side elements were duplicated and reflected to form the right

179 side of the skull. Transformation matrices for all bones from the original data set to the final 3D

180 reconstruction are available as supporting information (Appendix S2); a 3D PDF of the

181 reconstructed skull is also available as supporting information (Appendix S3).

182

183 **Institutional abbreviations**

184 BMT, Birmingham Museums Trust (encompasses BMAG, Birmingham Museum and Art

185 Gallery and TSM, Thinktank, Birmingham Science Museum), UK; BRLSI, Bath Royal Literary

186 and Scientific Institution, Bath, UK; BU, Lapworth Museum of Geology, University of

187 Birmingham, UK; LEICT, Leicester Arts and Museums Service, New Walk Museum and Art

188 Gallery, Leicester, UK; NHMUK, Natural History Museum, London, UK; SOMAG (formerly

189 AGC), Alfred Gillett Collection, cared for by the Alfred Gillett Trust (C & J Clark Ltd), Street,

190 Somerset, UK; UNM, University of Nottingham Museum, UK.

191

192 **Systematic Palaeontology**

193 Ichthyosauria de Blainville, 1835

194 Parvipelvia Motani, 1999

195 Ichthyosauridae Bonaparte, 1841

196 *Protoichthyosaurus* Appleby, 1979

197 *Protoichthyosaurus prostaxalis* Appleby, 1979

198

199 *Type species. P. prostaxalis* Appleby 1979. The type series of specimens are from historic

200 collections. However, the holotype is most likely from the area around Street, Somerset and is

201 most likely from the lowermost Jurassic (lower Hettangian) 'Pre-Planorbis Beds' (i.e., Tilmanni

202 Ammonite Zone) of the Blue Lias Formation, although it could be latest Triassic (Rhaetian). See

203 Lomax et al., (2017) for more details.

204

205   *Holotype*. BRLSI M3553, a partial skull, pectoral girdle, and both forefins, preserved in ventral

206   view.

207

208   *Paratypes*. BRLSI M3555, a skull and partial skeleton, preserved in right lateral view; BRLSI

209   M3563, a composite partial skeleton; LEICT G454.1951/164, a partial forefin, presently missing,

210   which might be a hindfin of a different genus (see Lomax, Massare & Mistry, 2017 for more

211   details).

212

213   *Referred specimen*. BMT 1955.G35.1, an almost complete, three-dimensional skull and partial

214   postcranial skeleton.

215

216   *Emended diagnosis*. As in Lomax et al., (2017), but with the following change: total length

217   greater than 3.2 m but probably less than 4 m.

218

219   *Occurrence*. Fell Mill Farm, between Shipston-on-Stour and Honington, Warwickshire, England,

220   grid reference NGR SP 277 415. The specimen was collected from blue-grey Liassic clay, and

221   specifically from the Semicostatum Ammonite Zone, lower Sinemurian, Lower Jurassic.

222

223   **Results**

224   *Anatomical description of the skull roof*

225   Measurements of the skull are presented in Table 1. In lateral view, the upper jaw is shaped like

226   a right-angle triangle, the ventral margin being nearly straight and dorsal surface of the snout

227   being gently sloped (Fig. 1). In dorsal and ventral views, the anterior snout (formed by the

228   premaxillae) is shaped like a finely pointed triangle (Fig. 2); the posterior portion of the skull is

229   transversely expanded. Preserved bones of the skull roof (Figs 1-2, 5) include most of the

230   premaxillae, both maxillae, partial nasals, partial left lacrimal, partial prefrontals and

231   postfrontals, complete left and partial right jugals, nearly complete parietals, and partial

232   supratemporals. Some of these elements (e.g. portions of nasal and postfrontals) were too

233   fragmentary and/or poorly preserved to attach to the skull and are not part of the 3D model. The

234   left postorbital was originally present (Fig. 1A), but we were unable to locate the element. The

235   quadratojugals and squamosals are not preserved in BMT 1955.G35.1. The frontals are also

236   missing with the exception of a small fragment attached to the left nasal. Unless otherwise stated,

237   the morphology concurs with other specimens of the species (Lomax, Massare & Mistry, 2017;

238   Lomax & Massare, 2018).

239

240   *Premaxilla*. The premaxilla makes up two-thirds of the length of the cranium and most of the

241   snout. The majority of both premaxillae are preserved, although portions of the posterior ends are

242   missing including the margin of the external naris (Figs 1-2). The left premaxilla is more

243   complete than the right element. In lateral view, the anterior premaxilla is dorsoventrally low but

244   becomes progressively taller posteriorly. A longitudinal groove exposing a series of foramina

245   (see below) along the lateral surface represents the fossa praemaxillaris (Figs 1B-C, 2). The right

246   premaxilla preserves a long, tapering subnarial process that articulates with the maxilla and

247   extends to the middle of the maxilla (Figs 1B, 2A); the supranarial process is not preserved on

248   either side. Laterally, the contact between the premaxilla and maxilla is clear and consists of an

249   extensive scarf joint in which the ventral margin of the premaxilla laterally and dorsally overlaps

250   the anterior process of the maxilla (Figs 1-2). The contact between the premaxilla and maxilla on

251 the palate is difficult to discern, although it appears that a maxillary shelf extends medially and

252 replaces the premaxillary shelf at the level of the 18th preserved tooth on the right side. (The

253 teeth, were reset during conservation and their positions in the jaw are not original. However,

254 their reconstructed positions act as landmarks for our description.) Except at the anterior tip of

255 the snout, the premaxillae do not meet at the ventral midline.

256   In dorsal view, the premaxillae would have contacted each other at a butt joint for much

257 of their length, although they are largely separated due to deformation (Fig. 2E). Posteriorly, the

258 nasals inserted between the premaxillae. The dorsal margin of the left premaxilla laterally and

259 dorsally overlaps the nasal from approximately the level of the 13th premaxillary tooth to its

260 broken posterior end. In dorsal view, a small, narrow portion of the anterior process of the nasal

261 is exposed; the rest is overlapped by the premaxilla.

262   Anteriorly, the premaxilla is a laterally bowed sheet of bone in transverse cross-section;

263 at the level of the seventh preserved tooth, it develops a medial shelf that roofs the alveolar

264 groove. From this point until its articulation with the maxilla, the premaxilla consists of a ventral

265 lamina that laterally overlaps the teeth, the medial shelf, and a dorsal lamina, which is deeply

266 grooved along its margin (as preserved on the right premaxilla), presumably to receive the nasal.

267 CT scans reveal that each premaxilla encloses a branching, longitudinal canal dorsal to the tooth

268 row (Fig. 2G-J). This canal extends from the posterior end of the premaxillary tooth row to the

269 third premaxillary tooth. Anteriorly, a series of short canals branch anterolaterally from the main

270 conduit and open onto the fossa praemaxillaris, either immediately above the alveolar margin or

271 on the dorsolateral aspect of the bone. The right premaxilla preserves five ventral and four dorsal

272 foramina; the left premaxilla preserves four ventral and one dorsal foramina. The posterior half

273 of each premaxilla contains two longer canals branching posteriorly from the main conduit, each

274   of which opens onto posteriorly elongated grooves parallel to the alveolar margin of the

275   premaxilla. The left premaxilla preserves two additional longitudinal grooves on the posterior

276   half of its dorsolateral surface; however, these do not connect to the main canal within the

277   premaxilla. These vascular canals within the premaxilla (as well as those within the dentary, see

278   below) resemble canals in the facial bones of extant crocodilians and lepidosaurs, as well as

279   those reported in theropod dinosaurs (Dal Sasso et al., 2009), pliosaurs (Ketchum & Benson,

280   2011; Foffa et al., 2014b), and plesiosaurs (Ketchum & Smith, 2010) and something similar in

281   ichthyosaurs (Lomax & Massare, 2015). In extant taxa, these canals carry neurovascular bundles

282   consisting of the maxillary artery and maxillary branch of the trigeminal nerve (CN V_2) in the

283   upper jaw, and the inferior alveolar artery and mandibular branch of the trigeminal nerve (CN

284   V_3) (Witmer, 1997). The complex web of ramifications reported in the upper jaw of pliosaurs

285   cannot be visualized in this specimen; this may be due to their absence, preservation or scan

286   resolution. Nonetheless, it is possible these canals were also associated with pressure or electro-

287   reception as seen in some extant taxa and as postulated for dinosaurs and pliosaurs (Foffa et al.

288   2014b).

289

290   *Maxilla*. Both maxillae are preserved, although the posterior portion of the left maxilla is missing

291   and both are damaged. In lateral view, the maxilla is a triangular bone with slender anterior and

292   posterior processes and is dorsoventrally tallest in its center (Figs 1-2). The anterior process is

293   longer and more delicate than the posterior process, which extends just under the orbit. Although

294   the external naris is not preserved, it is clear the maxilla extended well beyond the anterior end of

295   the external naris.

296   The alveolar groove of the maxilla is continuous with that of the premaxilla. In transverse

297   section, the anterior maxilla has a ventral lamina that extends lateral to the tooth row, a ventrally

298   curving medial shelf (forming the dorsal and medial walls of the alveolar groove) and a short

299   dorsal lamina that contacts the medial surface of the premaxilla in a scarf joint. The dorsal

300   lamina of the maxilla, which underlaps the premaxilla, is exposed slightly anterior to the middle

301   of the left maxilla due to the damaged premaxilla. Posterior to the main body, the maxilla is

302   triangular in transverse section with a ridge on its dorsomedial surface that appears to articulate

303   with the short anterior process of the lacrimal, which is poorly preserved. An articulation surface

304   on the dorsolateral surface of the posterior process of the maxilla meets the jugal in a scarf joint,

305   separating the posterior process of the maxilla from the lacrimal.

306

307   *Nasal*. The anterolateral portion of the left nasal is preserved attached to the premaxilla (Figs 1-

308   2). It is best seen in ventral and posterior views, which reveals it is dorsoventrally thickened

309   medially but becomes dorsoventrally thin laterally. The bone is laterally bowed in transverse

310   section. The ventral margin of the nasal is laterally overlapped by the dorsal lamina of the

311   premaxilla; the morphology of the right premaxilla suggests this may have originally been a

312   tongue-and-groove contact. Near the posterior end of the element is a small fragment featuring a

313   grooved medial margin; it is unclear if this is a portion of the nasal or a fragment of the frontal.

314   CT scans reveal a few short canals penetrating the nasal from its lateral surface.

315   Other fragments of the nasal were found with the specimen but not mounted on the skull

316   due to their fragile nature. Although very fragmentary, much of the right nasal is preserved

317   although the posterior end is missing and it is impossible to determine the presence of an

318   internasal foramen. It is a long and delicate element that is wide posteriorly, and tapers to a point

319   anteriorly (Fig. 5K-L). On the medial surface is a long groove that runs almost the entire length

320   of the nasal. The slightly flared lateral wing is damaged. Two foramina are present posteriorly,

321   positioned next to a portion of what may be the prefrontal.

322

323   *Lacrimal*. The left lacrimal is poorly preserved. It appears to be triradiate with a short, but

324   damaged anterior process and a longer posteroventral process. The dorsal process is tall and

325   formed the posterior margin of the external naris. It was clearly excluded from the orbital margin

326   by the anterior process of the prefrontal (Figs 1B, 2B,D). The lateral surface of the dorsal process

327   preserves external sculpting and several canals that penetrate the bone but cannot be traced. The

328   short, tapering anterior process fits onto a shelf on the dorsomedial aspect of the maxilla. The

329   posteroventral process, which is longer and mediolaterally wider than the anterior process, is

330   complete and contributes to the anteroventral margin of the orbit. It meets the dorsal margin of

331   the jugal in a curving contact. The lateral surface of the posteroventral process bears the remnant

332   of a ridge from its posterior tip to the base of the dorsal process.

333

334   *Prefrontal*. Only a small portion of the anterior process of the left prefrontal is present, although

335   original photographs of the mounted skull show that the element was once complete (Figs 1B,

336   2B). The anterior process of the prefrontal medially and dorsally laps the lacrimal along a broad

337   contact, where it is dorsoventrally tall and excludes the dorsal process of the lacrimal from the

338   orbital margin.

339

340   *Postfrontal*. The anterior portions of both postfrontals are preserved but were not added to the

341   mount. The right postfrontal is the more complete of the two elements (Fig. 5M). In dorsal view,

342   the anterior end is mediolaterally broad and dorsoventrally thin. The postfrontal narrows

343   posteriorly, where it is damaged. The medial surface exhibits a prominent ridge.

344

345   *Jugal*. The jugal is a long, slender bone forming the ventral margin of the orbit; the left is better

346   preserved than the right (Figs 1-2). Anteriorly it is oval-shaped in transverse section and tapers to

347   a point, contacting the posteroventral margin of the lacrimal and dorsolateral aspect of the

348   posterior process of the maxilla as previously described. Although damaged and perhaps missing

349   a small portion, it is clear the anterior process extended to at least the level of the anterior margin

350   of the orbit. Posteriorly, the dorsal ramus of the jugal gently curves dorsally, expands

351   dorsoventrally and thins mediolaterally. Based on the original reconstruction (Fig. 1A), which

352   featured a complete jugal and postorbital, the jugal contributed to about half of the posterior

353   orbital margin.

354

355   *Postorbital*. An original photograph shows that the postorbital was complete, but we have been

356   unable to locate the element (Fig. 1A). However, based on the photograph, it is clear that the

357   postorbital is dorsoventrally short and anteroposteriorly wide, being almost rectangular in shape

358   and making up half of the posterior orbital margin. The anterodorsal edge tapers to a narrow

359   process.

360

361   *Parietal*. Both parietals are damaged and missing their anteroventral margins, the left element

362   being better preserved (Figs 3, 5A-D). In dorsal view, the parietals are hour-glass shaped and

363   meet medially, diverging slightly anteriorly. CT scans reveal the dorsomedial margin of the

364   anterior parietal is strongly dorsoventrally expanded in transverse section, the elements

365   contacting each other at a tall midline butt joint; the parietal thins ventrolaterally in transverse

366   section. The articulation of the parietals results in a well-defined sagittal crest (Fig. 5A, C); at its

367   mid-section, the parietal is L-shaped in transverse section with the horizontal leg forming the

368   roof of the braincase while the ventral leg forms the lateral wall of the braincase and medial wall

369   of the supratemporal fenestra. Lateral to the crest, the dorsal surface of the parietal is convex and

370   curves ventrally, widening posteriorly. Posteriorly, the crest decreases in height to form an

371   extensive shelf (parietal ridge) under which the supraoccipital articulates (Fig. 5A, C). Two

372   elongate depressions, one on the posterior aspect of each parietal, may represent attachment sites

373   for epaxial neck muscles (Fig. 5C).

374   In ventral view, the surface of the parietal is concave and bears impressions of structures

375   that surrounded the brain (Fig. 5B, D). In the anterior region, impressions of the cerebral

376   hemisphere and extra-encephalic depression are present (as in McGowan, 1973). McGowan

377   (1973, fig. 48) showed that the cerebral hemisphere was present in both the parietal and frontal in

378   a specimen of *Ichthyosaurus*. In BMT 1955.G35.1, there is no indication of the frontal at this

379   position, suggesting the cerebral hemispheres were likely limited to the parietal. The descending

380   parietal flange is present in both parietals, although the left is more complete (Fig. 5B, D). The

381   anterior process is thick, short, and protrudes forwards, creating a ledge. Towards the center of

382   the parietal is the large, ovoid impression of the optic lobe, the most prominent of the cerebral

383   structures, situated posterior to the parietal flange (Fig. 5B). The epiterygoid process is not

384   preserved. Posteriorly, the parietal flares laterally to form the paraoccipital process; in posterior

385   view, this process is shaped like a bowtie and ventrally deflected. In ventral view, there may be

386   an impression of the cerebellum, although this is difficult to confirm because this portion is

387   damaged.

388

389 *Supratemporal*. Portions of both supratemporals are preserved. The majority is exposed at the

390 posterior margin of the skull, attached to the parietal (Figs 3C, 5C). It is difficult to identify the

391 parietal-supratemporal suture in the original specimen. In CT scans, the contact between the left

392 parietal and supratemporal is visible as a very tight, sinuous butt joint; this contact cannot be

393 discerned on the right and the two bones may have fused. In posterior view, the preserved

394 supratemporal is large and triradiate; it is narrow medially and increases in width distolaterally,

395 with a posteroventral process. In this view, it is roughened with numerous striae, probably for

396 muscle attachment (Kirton, 1983) (Fig. 5C). There are also some foramina present, similar to

397 those reported in this region of the supratemporal in ichthyosaurs such as the Cretaceous *Leninia*

398 *stellans* (Fischer et al., 2014).

399

400 *Anatomical description of the palate*

401 The left pterygoid, including a fragment representing the quadrate wing, and quadrate are

402 preserved (Fig. 3).

403 *Pterygoid*. The left pterygoid can be positively identified, although it is damaged. It is an

404 anteroposteriorly elongate element with a robust and mediolaterally wide posterior end and

405 narrow anterior end (palatal ramus) (Figs 3, 5E-F). The palatal ramus is dorsoventrally flattened

406 and makes up over half the length of the pterygoid; it is narrowest at its mid-length and expands

407 distally. Posteriorly, the pterygoid expands transversely and dorsoventrally to form the quadrate

408 ramus; its dorsal surface rises in a ridge that would have been continuous with the quadrate wing

409 (see below). Although damaged and incomplete, the overall morphology of this element,

410 particularly how the shape changes from the posterior end to the narrow mid-shaft which then

411   broadens anteriorly, is reminiscent to the pterygoid of *Sveltonectes* (Fischer et al., 2011, fig. 2G).

412   This differs from *Ichthyosaurus,* which has a very narrow shaft posteriorly (McGowan, 1973,

413   fig. 20), and from *Platypterygius longmani* Wade 1990 which has a mediolaterally wider shaft

414   (Kear, 2005, fig. 8C-E) and even from *Ophthalmosaurus icenicus* Seeley 1874, in which the

415   pterygoid has a distinctly different shape posteriorly (Moon & Kirton, 2016, plate. 6, figs 1, 2).

416   In dorsal view, the posterior end has three wing-like projections. The medial projection,

417   which is damaged and was originally more extensive, is the largest and most robust, whereas the

418   lateral projection is slender and dorsoventrally flattened (Fig. 5E). The ventral surface is better

419   preserved, although the edge of the interpterygoid vacuity is damaged (Fig. 5F). Regardless, the

420   posterior end of the pterygoid is larger, wider, and narrows more gradually than that of

421   *Ichthyosaurus* (McGowan, 1973, fig. 20B). The dorsal (quadrate) wing of the posterior ramus of

422   the left pterygoid is almost certainly represented by a large but thin fragment of bone, the shape

423   of which was obscured by a large amount of wood and plaster in the original reconstruction but

424   is revealed in CT scans.

425

426   *Quadrate*. Only the left quadrate is preserved, which is a large and robust element (Figs 3, 5G-I).

427   In anterior and posterior views the quadrate is C-shaped, owing to strong curvature of the shaft

428   (Fig. 5G-H); it is more of an L-shape in *Ichthyosaurus* (McGowan, 1973, fig. 9). The articular

429   condyle is massive and greatly expanded mediolaterally, whereas the dorsal end is mediolaterally

430   thin. A well-defined ridge is present above the condyle and displays a long groove identified as

431   the quadratojugal facet. A groove is present on the ventral surface of the condyle, which divides

432   the jaw joint surface into two distinct faces as is common among ichthyosaurs.

433

434   *Anatomical description of the braincase*

435   Preserved material includes the supraoccipital, left opisthotic, left stapes, and parabasisphenoid

436   (Fig. 3). The anterior portion of the parasphenoid as well as the basioccipital, prootics, and

437   exoccipitals are missing.

438   *Supraoccipital.* The median supraoccipital is triangular with its apex anterodorsally directed

439   (Fig. 6A-C). CT scans revealed that the right margin of the supraoccipital had been reconstructed

440   in plaster, obscuring the true shape of this element. In anterior and posterior views, the element is

441   convex and arch-like, and is wider than it is tall, which is similar in *Ichthyosaurus* (McGowan,

442   1973, fig. 4). Of particular note, in this view, the dorsal portion of the opening for the foramen

443   magnum is much more reduced than in either *Platypterygius longmani* (Kear, 2005, fig. 10D-E)

444   or *Ophthalmosaurus icenicus* (Moon & Kirton, 2016, Plate 9, fig. 1-5). A median ridge is present

445   on the posterior surface, which is sharpest anterodorsally and flattens as it approaches the

446   foramen magnum (Fig. 6B-C). This ridge would have contacted the parietal, as shown in the 3D

447   model (Fig. 3C, F) and separates two flat, posterolaterally-directed faces, each of which is

448   pierced by a canal that opens onto its internal surface (Fig. 3B, G). These openings probably

449   represent the foramen endolymphaticum (Andrews, 1910), which served for the passage of the

450   endolymphatic ducts (McGowan, 1973; Maisch, 2002; Marek et al., 2015) or veins (Kirton,

451   1983; Moon & Kirton, 2016). The complete left half preserves two articulation facets along its

452   ventral lateral margin – a larger, posteroventrally-directed facet that is deep and triangular-

453   shaped (apex pointing forward) and a smaller, oval-shaped facet that is posterolaterally-directed.

454   In dorsal view, there is a well-defined ridge that is separated by a long, trenchant groove

455   (Fig. 6B). For *Ichthyosaurus*, McGowan (1973, pg. 15) described the dorsal edge as having two

456   shallow grooves. The groove marks the boundary between the ossified and cartilaginous portions

457   of the neurocranium (McGowan, 1973). In ventral view, the element is arched with a smooth

458   section for the roof of the foramen magnum (Fig. 6C). The exoccipital facet is roughly square.

459

460   *Parabasisphenoid*. The thin parasphenoid is broken with a small portion preserved fused to the

461   basisphenoid (Fig. 6D). The basisphenoid is complete and is a large, robust element both

462   mediolaterally wide and dorsoventrally tall (Fig. 6D-E). There are deep grooves between the

463   posterior corners of the bases of the basipterygoid processes and the main body for the palatal

464   ramus of the facial nerve (Kirton, 1983). In dorsal view, the midline of the anterior end is convex

465   and, along with the protruding anterior ends of the basipterygoid processes, gives the anterior

466   margin of the basisphenoid a 'three-pronged' appearance, resembling a specimen of

467   *Ichthyosaurus* referred to as the 'Evans Nodule' by McGowan (1973, plate 1a). The

468   basipterygoid processes are both complete, robust and oblong in ventral view (Fig. 6E). Their

469   surfaces appear slightly roughened, probably due to a cartilaginous covering for contact with the

470   pterygoid. The distal articular facet of the basipterygoid process is defined by a depression with a

471   rim. The anterior tip of the basipterygoid process is tapered, whereas the posterior margin is

472   thickened and rounded.

473   The anterodorsal aspect of the basisphenoid features a pair of robust protuberances

474   separated by a slight midline depression – the sella turcica – that housed the pituitary gland (Fig.

475   6D). Below this is the median opening for the carotid artery, which courses posteroventrally

476   through the bone and exits on its ventral surface as a rounded opening bounded proximally by an

477   arch-like ridge (Fig. 6D-E). Ventral to this opening and dorsal to the parasphenoid is a kidney-

478   shaped articulation facet, interpreted as the impressions of paired trabeculae (as in McGowan,

479   1973, fig. 1) (Fig. 6D). Immediately dorsal and posterior to the sella turcica, is a large, bulbous

480   region that has the ossified dorsum sellae (dorsal crest). The posterior surface is a wide, rounded

481   rectangle, indented for reception of the basioccipital.

482

483   *Opisthotic*. Only the left opisthotic could be identified (Fig. 6F-G). It is a robust and stout

484   element that is roughly pentagonal in posterior view. Its ventrolateral margin is long and sharp.

485   Ventrally the opisthotic tapers to a point that bears a small facet, which articulates with the

486   stapes. The stapedial facet is large, but the lateral 'foot' (after Fischer et al., 2012) has minor

487   exposure. The ventromedial margin is concave and bears a long, low groove that marks the

488   basioccipital facet (Fig. 6G). The dorsolateral margin forms the prominent paroccipital process,

489   the posterior surface of which bears a long, prominent ridge that ascends vertically from the

490   ventral tip of the element, then turns medially. A deep groove, for either the glossopharyngeal or

491   branch of the facial nerve (Kirton 1983; Marek et al., 2015), separates this ridge from a

492   pronounced protuberance on the dorsal margin of the opisthotic. The dorsomedial margin is

493   expanded into a rugose, subtriangular depression (apex pointing posterodorsally) surrounded by

494   a raised lip and several small protuberances. Although poorly preserved, the membranous

495   impressions of the posterior vertical semicircular canal, sacculus, the horizontal semicircular

496   canal and possibly utriculus are represented by a somewhat 'V-shaped' impression, best

497   observed in anteromedial aspect (Fig. 6F). The impression of the horizontal semicircular canal is

498   damaged at the tip and the impression of the sacculus is wide and round. There are several

499   grooves positioned adjacent to the impressions, which McGowan (1973, fig. 5) referred to as

500   grooves in the margin circumscribing the membranous impression. Computed tomography

501   reveals a great deal of trabecular bone within the opisthotic.

502

503 *Stapes*. Both stapes are preserved, with the left being more complete. The stapes is

504 mediolaterally elongate with a bulbous occipital head and a tapered distal end (Fig. 6H). The

505 proximodorsal region of the medial head bears a groove that marks the course of the stapedial

506 artery. In anterior view, the medial head is laterally inclined and there is a shallow groove, which

507 is probably the opisthotic facet. The posterior surface of the stapes bears a series of oblique

508 ridges and grooves. This may have been an area for muscle attachment (McGowan, 1973, fig.

509 7a) (Fig. 6H). There are several small canals within the stapes; however, these are very difficult

510 to trace.

511

512 *Anatomical description of the lower jaw*

513 Nearly complete left and right dentaries are present, as are both incomplete splenials, the nearly

514 complete left surangular, and the complete left articular and angular (Fig. 4).

515

516 *Dentary*. The dentary makes up over three-quarters the length of the lower jaw. It is elongate,

517 tapering at its anterior and posterior ends (Figs 1, 4). The ventral margin is convex while the

518 dorsal margin is concave, and the entire element curves dorsally at its anterior end; the latter is

519 likely the result of taphonomic distortion. As with the upper jaw, the lower teeth have been reset

520 in a continuous groove, which we use as landmarks for our description. In transverse section, the

521 anterior dentary is roughly oval-shaped with a convex lateral surface; a medial shelf forms the

522 floor of the alveolar groove and a dorsal lamina laterally overlaps the dentary teeth. The medial

523 shelf is separated from a longitudinal ridge that parallels the ventral margin of the bone by a

524 shallow groove (lateral wall of the Meckelian canal); this ridge and groove dominate the internal

525 face of the anterior half of the dentary. At the level of the 15th dentary tooth, the medial shelf

526   disappears and the dentary becomes a laterally bowed sheet of bone with a thickened dorsal

527   margin in transverse section.

528   The anterior tip of the right dentary is damaged and, as a result, the dentaries do not

529   contact each other anteriorly to form the mandibular symphysis (Figs 1, 4). As preserved, the

530   dentary and splenial do not contact each other along their entire length but this is due to

531   distortion. The anterior tip of the angular is level with the 17th preserved tooth on the right side;

532   the angular laterally overlaps the ventral margin of the dentary in a very tight scarf joint. In

533   contrast, the suture between the dentary and surangular, which reaches the level of the 22nd

534   preserved dentary tooth, is a loose, horizontal butt joint except at its posterior end where the

535   posterior tip of the dentary laterally overlaps the surangular.

536   As with the premaxilla, CT scans reveal that each dentary encloses an elongate,

537   branching canal ventral and lateral to the tooth row that extends from the anterior tip of the bone

538   to the 14th (right) and 9th (left) preserved dentary teeth, at which point the canal opens onto the

539   internal surface (Meckelian canal) of the lower jaw ventral to the medial shelf of the dentary

540   (Fig. 4C, G-J). Anteriorly, four small canals branch laterally from the main conduit and open

541   onto short, posteriorly elongated grooves on the lateral face of the dentary. A posterior (fifth)

542   canal opens into a very long groove ventral and parallel to the tooth row that extends over a

543   quarter the length of the dentary.

544

545   *Splenial*. The splenial is composed of a vertical sheet of bone that is medially concave, a slightly

546   thickened dorsal margin that is turned medially, and a thickened, laterally deflected ventral

547   margin. Thus, the element has a mild S-shape and is mediolaterally thin in transverse section

548   anteriorly, becoming more robust with increasingly pronounced curvature posteriorly. The

549   splenial forms the medial wall and part of the floor of the Meckelian canal for the posterior half

550   of the lower jaw. Its contacts with other elements cannot be reliably interpreted as the bones

551   were not in articulation; however, from their preserved ventral margins, it appears the splenial

552   and angular met in a butt joint.

553

554   *Angular*. The angular extends over half the length of the lower jaw (Figs 1, 4B). The anterior half

555   of the angular is a long, straight rod while the posterior half is both dorsoventrally and

556   mediolaterally expanded, curving dorsally and medially towards the jaw joint. In transverse

557   section, the anterior half of the angular is diamond-shaped with a dorsomedial surface that

558   contacts the ventral margin of the dentary in a tight scarf joint and a dorsolateral surface that

559   meets the ventral margin of the surangular in a loose butt joint. The ventromedial surface of the

560   anterior angular bears a shallow, longitudinal groove bounded dorsally and ventrally by low

561   ridges that presumably articulated with the splenial. Posteriorly, the angular develops a robust

562   tab or lamina that extends from its dorsomedial surface and medially laps the surangular.

563   However, immediately ventral to the jaw joint, this lamina disappears and is replaced by taller,

564   mediolaterally thin dorsolateral lamina that extensively overlaps the lateral aspect of the

565   posterior surangular. Thus, the contact between the angular and surangular is morphologically

566   simple and loose anteriorly but tighter and more complex posteriorly. In lateral view, the anterior

567   end of the surangular is broken and it appears the angular extends further anteriorly than the

568   surangular (Fig. 4B). This is similar to specimen SOMAG 12, a referred specimen of

569   *Protoichthyosaurus prostaxalis* (Lomax, Massare & Mistry, 2017).

570

571 *Surangular*. The surangular is a long, curved element forming the lateral aspect of the posterior

572 third of the lower jaw (Figs 1, 4B). The anterior half of the surangular is poorly preserved as it is

573 mediolaterally thin and is loosely joined to the dentary (dorsally) and angular (ventrally) via

574 rounded butt joints. Posterior to the dentary, the dorsal margin of the surangular thickens

575 dramatically to form the peaked coronoid process. A longitudinal lateral ridge, dorsally bounding

576 the fossa surangularis, continues to the end of the surangular and separates the thickened dorsal

577 margin from the thinner ventral lamina that articulates with the angular. The element expands

578 dorsally and medially at its rounded posterior end to laterally cup the articular.

579   In medial view, the posterior surangular bears a ridge parallel to its ventral margin that

580 articulates with the angular and forms the floor of the adductor fossa. There is another, more

581 robust ridge on the medial surface originating at the coronoid process and widening posteriorly

582 to contact the anterior surface of the articular. The medial face of the surangular between the two

583 ridges is concave and forms the Meckelian groove and lateral wall of the adductor fossa. There is

584 a large foramen clearly visible on the medial aspect ventral to the coronoid process; this foramen

585 passes laterally through the surangular and exits ventral to the ridge on the lateral surface (Fig.

586 4D, K).

587

588 *Articular*. The preserved left articular has a triangular profile in dorsal and ventral views, with

589 the apex posteriorly and medially directed, and a subcircular profile in medial and lateral views.

590 The posterior margin is sharp while the anterior aspect is flat and broad where it contacts the

591 quadrate to form the jaw joint. The medial aspect of the bone is smooth while the lateral aspect is

592 pitted and porous. CT scans reveal several small, short canals that penetrate into the bone from

593 its lateral surface.

594

595 *Hyoid*. Both hyoids are preserved and are large and complete, although some damage is

596 apparent. The hyoid is a curved, rod-like bone (Fig. 5J). In dorsal view, the element is slightly

597 bowed posterolaterally and the center of the element is slightly mediolaterally narrower than

598 either end. The anterior end is slightly flattened, rounded and pitted for reception of cartilage. In

599 anterior view, the probable left hyoid is oval-shaped, with a defined rim.

600

601 *Dentition*. The teeth were implanted in an aulacodont fashion in continuous alveolar grooves as

602 is typical in euichthyosaurs. As previously mentioned, the teeth were not preserved in situ and

603 were added to the grooves during reconstruction of the skull both in 1955 and in 2015; thus, they

604 are not in their original positions. Furthermore, the dental groove is too poorly preserved to

605 determine the exact number of teeth that would have originally been present. There are

606 additional fragmentary and complete teeth associated with the specimen.

607   The teeth are lingually curved, large cones with short, robust crowns with fine striations

608 and smooth apices (Figs 1B-C, 5N). In complete teeth, the crown is much narrower than the root.

609 The roots are large with prominent longitudinal grooves that extend to the base of the crown and

610 continue as longitudinal striations on the crown (Fig. 5N). This morphology is found in all

611 specimens of *Protoichthyosaurus* that have well-preserved teeth (Lomax, Massare & Mistry,

612 2017; Lomax & Massare, 2018). Tooth morphology for each tooth is similar, with crowns

613 ranging from 0.87 cm to 1.75 cm in height. As no teeth were preserved in situ, it is impossible to

614 differentiate between the premaxillary, maxillary and dentary teeth. A resorption pit is present on

615 the lingual surface in many teeth (e.g. Fig. 5N). CT scans reveal hollow pulp cavities within the

616 teeth that open at the tooth bases and extend nearly the entire height of the tooth.

617

618   *Anatomy of the postcranial skeleton.*

619   Portions of the vertebral column, ribs, gastralia, forefin, pectoral girdle, pelvic girdle and the

620   hindfin are preserved (Fig. 7). The forefin and hindfin phalangeal elements are entirely free of

621   matrix and are not in their original context, so it is impossible to say whether elements are from

622   the left or right fin.

623

624   *Axial skeleton.* A total of 37 vertebral centra are present, all of which are disarticulated. Most are

625   poorly preserved but their positions in the column can be identified from their morphology. One

626   centrum is unusual in possessing the following features: triangular in anterior and posterior

627   views; being marginally anteroposteriorly longer than the preserved cervicals; diapophyses and

628   parapopthyses being high and positioned at the anterior end of the centrum in lateral view; two

629   separate semi-circular facets for articulation with intercentra in ventral view (Fig. 7A-B). This

630   morphology is indicative of an atlas-axis complex, but the centrum displays no fusion. This is

631   unusual given that, with the possible exception of immature individuals and some early Triassic

632   taxa, the atlas-axis is always fused in ichthyosaurs (McGowan & Motani, 2003; VanBuren &

633   Evans, 2017). The presence of two facets on the ventral surface might suggest that this element is

634   the atlas, with the diagonally-oriented anterior facet being for the atlantal intercentrum and the

635   posterior facet for the axial intercentrum (Fig. 7B). Alternatively, and more likely, this is the

636   axis, with the anterior facet being for the axial intercentrum and the posterior facet being for the

637   intercentrum of the third cervical vertebra (McGowan & Motani, 2003, fig. 5C). Interestingly,

638   the anterior surface of the axis centrum is not well-defined, nor smooth and lacks the convexity

639   typical of ichthyosaur centra (Fig. 7A). This might be pathological or it could be the surface that

640   was fused with the atlas vertebra that is not usually preserved (or exposed). A second centrum

641   features similar morphology but is slightly anteroposteriorly shorter and has only one small,

642   anterior facet on the ventral surface, which articulates with the aforementioned vertebra. It is

643   likely that this is the centrum of the third cervical vertebra. The remaining vertebral centra

644   include 19 dorsals, including elements from the anterior, middle and posterior portions of the

645   series as identified by their shape and position of the diapophyses and parapopthyses, and 16

646   caudal vertebra, again including elements from the anterior, middle and posterior portions of the

647   series as identified by their shape and the presence of a single rib facet.

648   One isolated and damaged neural spine, which is mediolaterally thin at its distal end, is

649   preserved.

650   Numerous incomplete ribs and rib fragments are preserved. The cross-sectional geometry

651   of the ribs varies, with some being rounded whereas others have a dumbbell-shaped cross

652   section. A possible gastralia fragment is present, which is roughened at its anterior end where it

653   presumably met its counterpart at the midline.

654

655   *Pectoral girdle*. The left coracoid is practically complete (Fig. 7C). It is a robust element that is

656   slightly anteroposteriorly longer than mediolaterally wide (Table 1). It has prominent and well-

657   developed anterior and posterior notches. The anterior notch is wider than the posterior notch,

658   resulting in the posterior end of the coracoid being mediolaterally wider than the anterior end. A

659   prominent rim outlines the glenoid and scapular facets, the former being noticeably longer than

660   the latter. In medial view, the intercoracoid facet is dorsoventrally thickened and bulbous at the

661   anterior end but narrows posteriorly.

662   Only the left scapula is preserved and is missing its posterior end (Fig. 7D). The

663   anterodorsal end is marked by a right angle, which extends to the ventral edge. This proximal

664   end is twice as tall dorsoventrally as the mid shaft and is widely flared but without a prominent

665   acromion process.

666

667   *Forefin*. As mentioned previously, none of the phalangeal elements were found in articulation. It

668   is impossible to determine whether the elements are from the left or right fin or determine the

669   morphology of the forefin in this specimen. The radius and ulna are missing and the preserved

670   elements are polygonal. Of note, the forefin was reconstructed for display in 1955 and 2015 with

671   the morphology typical of *Ichthyosaurus* (Motani, 1999). This was prior to the resurrection of

672   *Protoichthyosaurus* (Lomax, Massare & Mistry, 2017).

673   A single, nearly complete left humerus is robust, elongate, and slightly wider distally than

674   proximally without a prominent constriction in the mid shaft (Fig. 7E-F). It is the largest

675   humerus of *Protoichthyosaurus* described thus far (Table 1). The proximal end is large, bulky

676   and the surface is rugose and roughened. In ventral view, the deltopectoral crest is offset

677   anteriorly and is large but does not extend far down the shaft. The base of the anterior end is

678   slightly flared due to the presence of an anterior facet. The dorsal process is broken but appeared

679   centrally located. There are several possible predation marks preserved on the ventral surface of

680   the humerus (Fig. 7F). The facets for the radius and ulna are also damaged.

681

682   *Pelvic girdle*. A single ilium is well-preserved (Fig. 7G). It is a relatively thick and elongate

683   element that is J-shaped in lateral and medial views, resembling the ilium of *Ichthyosaurus*

684   *somersetensis* in being more oblong than rib-like (Lomax & Massare, 2017). The presumed

685   posterior end is slightly bulbous, relative to the shaft, somewhat similar to the ilium of

686   *Protoichthyosaurus applebyi* (Lomax, Massare & Mistry, 2017, UNM.G.2017.1). The presumed

687   anterior end is highly rugose. A possible ischium might also be preserved, but it is heavily

688   damaged.

689

690   *Hindfin*. Like the forefin, some phalanges of the hindfin are preserved, which are largely

691   polygonal, but none were found in articulation and all have lost their original context.

692   Regardless, the single, incomplete femur provides information (Fig. 7H-I). As the proximal end

693   is poorly preserved, it is difficult to identify the element as being from the left or right, but it is

694   most likely a right femur, based on the following comments. It has a very slender shaft, narrow

695   proximal end, and a flared distal end. Both the dorsal and ventral processes are damaged and

696   worn, but the supposed dorsal process seems to be a prominent, narrow ridge and the supposed

697   ventral process is large. There is a slight flare at the anterior end, but the posterior end is only

698   slightly expanded, and is almost a right angle. The tibial facet is larger than the fibular facet.

699

700   *Historically modelled regions of the skull of BMT 1955.G35.1*

701   CT-scanning the skull of BMT 1955.G35.1 aided substantially in our anatomical description.

702   Additionally, modelled areas of the skull can be clearly differentiated from fossil bone in scans

703   by the differing densities of these materials (Fig. 8). Fossil bone is the densest material

704   (appearing as bright areas within CT scans) followed by regions of the braincase that were 3D

705   printed in gypsum (see Material and Methods). Areas of the skull modelled during its initial

706   reassembly post-May 1955 are the least dense, as they are either composed of wood or a

707   traditional mix of alvar, jute and kaolin (known as AJK dough). Some modelled areas – such as

708   the posterior third of the right lower jaw, central portion of the right jugal, and "symphysis"

709   between left and right dentaries – are immediately apparent. Other areas, including the right

710   lacrimal and prefrontal, and various patches in the lower jaws, are less obvious. The skillfully

711   modelled right margin of the supraoccipital is only evident in CT scans, as are portions of the

712   braincase that were 3D printed and added to the newly reassembled skull. Thus, our work

713   demonstrates the utility of applying CT scanning to older, potentially modified museum

714   specimens to better understand both anatomy and specimen history.

715

716   *3D digital reconstruction of the skull of BMT 1955.G35.1*

717   Limits to the data set used in the 3D digital reconstruction of the skull must be noted. Numerous

718   bones are absent, fragmentary or were too delicate to scan, and some aspects of the 3D

719   reconstruction are uncertain. For example, the width of the reconstructed skull is constrained by

720   the articulation of the premaxillae (anteriorly) and contacts between the basisphenoid, pterygoids

721   and quadrate (posteriorly). Bones of the skull roof and palate that determine width in the middle

722   part of the skull are missing. Furthermore, the placement of the preserved bones of the posterior

723   skull roof is an estimate based on 1) the predicted height of the missing exoccipitals relative to

724   other braincase elements, and 2) the assumption of a smooth slope between the nasals and

725   parietals, as observed in other large ichthyosaurs, including examples of the genus

726   *Protoichthyosaurus* (Lomax, Massare & Mistry, 2017; Lomax & Massare, 2018). We did not

727   attempt to retrodeform elements that experienced plastic deformation, specifically the lower

728   jaws. The exaggerated dorsal and lateral curvature of these elements prevents complete closure

729   of the upper and lower jaws in our model. Similarly, the premaxilla and nasals could not be

730   completely re-articulated due to their deformed nature. Thus, this 3D digital reconstruction is our

731   current best hypothesis of the original skull shape of BMT 1955.G35.1 based on preservation and

732   personal interpretation. With these limitations in mind, the digital reconstruction nonetheless

733   yields useful new information on overall skull shape in this taxon (Fig. 9; Appendix S3). This

734   skull shape is typical of *Protoichthyosaurus prostaxalis* in lateral view (Fig. 9A), in having a low

735   skull that is slightly inclined from the nasals to the posterior end of the skull and in possessing a

736   relatively long and slender rostrum especially when compared with Lomax et al., (2017, figs. 2C,

737   4A-B) and Lomax and Massare (2018, figs. 2–3).

738   Due to the limitations of the fragile nature of the specimen some of the bones could not

739   be articulated in life position in the physical model and there are differences between the digital

740   and physical (Figs. 1, 2; Appendix S1) models. Of note, the rear of the skull is mediolaterally

741   wider and dorsoventrally shorter in the digital reconstruction than in the physical model. This is

742   due to placement of the basisphenoid dorsal and anterior to its true articulation with the

743   pterygoids in the physical model, as well as midline contact between the pterygoids; the

744   pterygoids are separated by the basisphenoid in ichthyosaurs (McGowan, 1973, Kirton, 1983;

745   Kear, 2005). The stapes is dorsally displaced in the physical reassembly; in other ichthyosaurs,

746   the stapes contacts the quadrate dorsal to its expanded base (Andrews, 1910; Kirton, 1983;

747   McGowan & Motani, 2003). Lastly, the jugal extends posterior to the quadrate in the physical

748   model, leaving no space for the posterior facial bones and resulting in the upper jaw being

749   anteroposteriorly shorter than the lower jaw. Shifting premaxilla and contacting bones so that the

750   anterior tips of the premaxillae and dentaries are level results in a gap between the jugal and

751   quadrate large enough to accommodate the missing postorbital and quadratojugal. These

752   differences highlight another advantage of applying 3D imaging and visualization methods to

753   large specimens. Large fossil bones are fragile and heavy, and there are practical limitations to

754 how they can be physically manipulated and mounted when reassembling a skull or skeleton;

755 digital manipulation of fossil bones reduces risk to the specimen and errors can be easily

756 corrected.

757

758 **Discussion**

759 BMT 1955.G35.1 has never formally been described. The original museum record shows that it

760 was initially identified as *Ichthyosaurus communis*, a species to which many ichthyosaur

761 specimens were historically referred as it is among the most common ichthyosaurs in the UK

762 (but see Massare & Lomax, 2017). In notes held at the Warwickshire Geological Records

763 Service (pers. comm. J. Radley, 2015), a report by Dr Brian Seddon, stated: "It is believed that

764 this animal is a new species lying somewhere between communis [*I. communis*] and breviceps [*I.*

765 *breviceps*]". A 1957 letter from Seddon states that it was ichthyosaur expert Robert Appleby who

766 expressed the opinion that the specimen possibly represented a new species and requested photos

767 be taken. More recently, Larkin et al. (2016) tentatively identified the specimen as

768 *Ichthyosaurus,* based on available information at the time. Since then, a revised diagnosis of

769 *Ichthyosaurus* has been published (Massare & Lomax, 2017), along with a redescription of

770 *Protoichthyosaurus* (Lomax, Massare & Mistry, 2017), a genus first described by Appleby

771 (1979), which was later synonymized with *Ichthyosaurus* (Maisch & Hungerbühler, 1997).

772   Lomax et al. (2017) provided an emended diagnosis of *Protoichthyosaurus*, which

773 included several autapomorphies of the forefin. Lomax and Massare (2018) provided additional

774 information on the genus and species, including a revised diagnosis, and showed that the genus

775 can also be distinguished from *Ichthyosaurus* by a combination of skull characters. They further

776 noted that characters used to distinguish individual species of *Protoichthyosaurus* from

777   individual species of *Ichthyosaurus* are more easily evaluated. The forefin of BMT 1955.G35.1

778   is entirely reconstructed and we have been unable to locate photographs or illustrations of how

779   the freshly excavated forefin appeared. Thus, the forefin cannot be used to identify the specimen.

780   BMT 1955.G35.1 does possess features shared by both *Ichthyosaurus* and

781   *Protoichthyosaurus*, including: a coracoid with both prominent anterior and posterior notches;

782   scapula with a narrow shaft that is expanded at the anterior end, but without a prominent

783   acromion process; a humerus with nearly equal width distally and proximally, with only a slight

784   constriction in the shaft; and femur longer than wide, with distal end wider than proximal end.

785   BMT 1955.G35.1 can, however, be assigned to *Protoichthyosaurus* on the basis of several

786   characters. Some of these characters are also found in some species of *Ichthyosaurus* but not in

787   the same combination (Lomax & Massare, 2018). They include: the prefrontal anterior process

788   separates the lacrimal dorsal process from the orbit margin; strongly asymmetric maxilla with

789   long, slender anterior process; teeth that have large roots with deep, prominent grooves that

790   extend to the base of the crown and are continuous with the ornamentation of the crown itself;

791   and a long, slender rostrum. In addition, the slightly diverging anterior end of the parietals in

792   BMT 1955.G35.1, which leaves an opening at the anterior end, is indicative of the posterior

793   opening for the pineal foramen between the parietals and frontals. Because the frontals are not

794   preserved, it is not possible to confirm if this is correct, but it seems plausible as this is the

795   position of the pineal in *Protoichthyosaurus* (Lomax & Massare, 2018). In *Ichthyosaurus* the

796   pineal is between the frontals and parietals (Massare & Lomax, 2017).

797   *Protoichthyosaurus prostaxalis* and *P. applebyi* differ in skull and humeral morphologies

798   (Lomax, Massare & Mistry, 2017). A third questionable species, *P. fortimanus*, known only from

799   an isolated forefin missing the humerus, displays only characters of the genus (see discussion in

800   Lomax & Massare, 2018). The left humerus of BMT 1955.G35.1 is damaged on its dorsal

801   surface. This restricts its usefulness in identification because the two species can be

802   differentiated by the dorsal process, which is missing in this specimen. The humerus of BMT

803   1955.G35.1 is robust, more similar to *P. prostaxalis* than *P. applebyi*, but this may be due to the

804   large size of BMT 1955.G35.1 (see Lomax, Massare & Mistry, 2017, fig. 5). However,

805   considering the size, Lomax and Massare (2018) recently described the second known specimen

806   of *P. applebyi*, an isolated skull (NHMUK R1164), which is comparable in size with some

807   smaller specimens of *P. prostaxalis*. They identified NHMUK R1164 as probably an adult and

808   showed that the differences among the two species are not ontogenetic. BMT 1955.G35.1 is

809   more than twice the size of NHMUK R1164 and is probably an adult *P. prostaxalis*.

810   Unfortunately, BMT 1955.G35.1 is missing some features of the skull that distinguish the two

811   species. However, the maxilla of BMT 1955.G35.1 is large, triangular, dorsoventrally high, and

812   possesses a long and narrow anterior process that is longer than the posterior process. In *P.*

813   *applebyi*, the maxilla is dorsoventrally low. Furthermore, although the jugal is incomplete and

814   the postorbital is missing, they were complete and part of the original mount (Fig. 1A). The

815   morphology of the postorbital, although based on the interpretation of a photograph, in being

816   dorsoventrally short but anteroposteriorly wide almost rectangular, and making up half of the

817   posterior orbit margin are characters found in *P. prostaxalis* (Lomax, Massare & Mistry, 2017;

818   Lomax & Massare, 2018). In *P. applebyi*, the postorbital is dorsoventrally long, anteroposteriorly

819   narrow, and makes up much more than half of the orbit posterior margin (Lomax & Massare,

820   2018). Consequently, even accounting for a misinterpretation of the postorbital morphology, its

821   shape does not match what is found in *P. applebyi*. Thus, based on the morphology and extent of

822   the maxilla and postorbital, we assign the studied specimen to *P. prostaxalis*. The difference in

823   size between the studied specimen and the presumed adult specimen of *P. applebyi* (NHMUK

824   R1164) is another indicator that the studied specimen belongs to *P. prostaxalis*.

825   It should also be noted that the maxilla of BMT 1955.G35.1, although dorsoventrally

826   high, does not appear as tall as in some specimens of *P. prostaxalis* (e.g. BRLSI 3555, BU

827   5323), but this is due to damage to the dorsal lamina of the maxilla on both sides. It may also

828   appear shorter due to the length of the studied skull, which is almost twice that of the largest

829   reported specimen of *P. prostaxalis* (Lomax, Massare & Mistry, 2017; Lomax & Massare, 2018),

830   with an estimated total skull length of at least 80 cm and estimated mandible length of 87 cm.

831   This is also much larger than the sister taxon *Ichthyosaurus*, with maximum skull and mandible

832   lengths of 57.5 cm and 67 cm respectively (Lomax & Sachs, 2017). Considering that the skull

833   length is approximately 20-25% of the total body length, based on a paratype specimen of *P.*

834   *prostaxalis* (BRLSI M3555), we estimate BMT 1955.G35.1 would have been between 3.2 and 4

835   m in length. This is the largest example of the genus known, the previous total length estimate

836   being 2.5 m (Lomax, Massare & Mistry, 2017). The largest unequivocal example of

837   *Ichthyosaurus* has a maximum total body length estimate of 3.3 m (Lomax & Sachs, 2017), thus

838   the maximum length estimate of the specimen described herein is also larger than all known

839   examples of *Ichthyosaurus*.

840

841   **Conclusions**

842   In this study, we describe a large, partial ichthyosaur skeleton from the Early Jurassic of

843   Warwickshire, England. In addition to examining the specimen, we carried out CT scanning of

844   individual skull bones as well as the entire, reassembled skull, one of the first times the skull of a

845   large marine reptile has been successfully CT-scanned, visualized and reconstructed in 3D (see

846   McGowan, 1989; Foffa et al., 2014a). CT scanning contributed greatly to our anatomical

847   description by revealing features not visible on original fossil material such as: branching,

848   longitudinal vascular canals within the premaxilla and dentary; short canals penetrating the nasal,

849   lacrimal, stapes, and articular; trabecular bone within the opisthotic; canals in the basisphenoid

850   and supraoccipital; the presence of the quadrate process of the pterygoid; and the sutural

851   morphology. We also demonstrate the utility of applying medical imaging techniques to historic

852   specimens to differentiate between original fossil material and reconstructed regions, as well as

853   the advantage of using digital visualization to accurately reconstruct large fossil specimens in

854   3D.

855   The detailed description of the three-dimensional skull and braincase presented herein

856   also provides information that can be used in phylogenetic studies. Although incomplete, the

857   skull and braincase preserve various elements that have not previously been reported or

858   described in any specimen of *Protoichthyosaurus* and therefore it provides more information

859   about this taxon so that its phylogenetic position can be explored in more detail. Furthermore,

860   our study has found additional characters that may lend further support for the distinction of

861   *Protoichthyosaurus* from its sister taxon *Ichthyosaurus*, such as the morphology of the pterygoid

862   and anteroventral surface of the parietal, which differ from that described for *Ichthyosaurus*

863   (McGowan, 1973). However, considering that only a couple of specimens preserve these

864   elements, it is possible that the differences may be the result of individual variation; more three-

865   dimensional specimens of both taxa are needed to test and clarify these findings.

866   Based on a unique combination of characters, we identify the specimen as

867   *Protoichthyosaurus prostaxalis*. With a skull nearly twice as long as any previously described

868   specimen of *P. prostaxalis,* this specimen greatly increases the known size range of this genus.

869 Compared with known, contemporaneous Sinemurian ichthyosaurs, the estimated size suggests it

870 was larger than all species of *Ichthyosaurus* (Lomax & Sachs, 2017), and comparable with the

871 largest known specimens of *Leptonectes tenuirostris* (McGowan, 1996a), but smaller than

872 *Leptonectes solei* (McGowan, 1993), *Excalibosaurus costini* (McGowan, 2003) and

873 *Temnodontosaurus platyodon* (McGowan, 1996b). Thus, our study also provides new

874 information on ichthyosaur diversity and potential ecology in the Early Jurassic of the UK.

875

876 **Acknowledgements**

877 Firstly, we would like to thank Luanne Meehitiya (formerly of TSM) who first discussed BMT

878 1955.G35.1 with NRL and DRL, and provided access to study the specimen. We would like to

879 express our thanks to each of the funders, which led to the scientific study and description of the

880 specimen. Thanks to Marta Fernández, Benjamin Moon and Alfio Chiarenza for their thorough

881 and constructive reviews of this manuscript, which were greatly appreciated. We also thank

882 Lukas Large (TSM) for assistance and the Birmingham Museums Trust for the photos

883 reproduced in Figure 1B and 1C. Judy Massare and Valentin Fischer are acknowledged for

884 helpful comments on the morphology of the skull. Jon Radley provided information on the

885 geology of the site and records relating to the excavation. David Ward identified the shark tooth

886 and provided stratigraphic information about the species. Michael Howarth identified the

887 ammonite associated with the postcranial skeleton and the ammonites recently collected by NRL

888 from the original site. The current landowner R. E Morley and the tenant farmer Robert Heath

889 gave permission for large holes to be dug at the site and Malcolm Bryan and Sally Bryan (son

890 and wife of the original finder of the specimen, Michael Bryan) and Clive Jeffries assisted with

891 the fieldwork. Robert Asher and Colin Shaw (University of Cambridge) provided access to

892 microCT-scanning facilities; Renate Weller (Royal Veterinary College) carried out CT-scanning

893 of the full skull. Technical support for Avizo was provided by Alejandra Sánchez-Eróstegui and

894 Jean Luc-Garnier (Thermo Fisher Scientific). Steven Dey (ThinkSee3D) mirrored microCT data

895 and 3D printed the missing bones on the right side of the skull.

896

897 **Data and Materials**

898 Original CT data of the full skull is available at MorphoSource, here:

899 https://www.morphosource.org/Detail/MediaDetail/Show/media_id/29156. Raw microCT data

900 of individual braincase elements is not available as these data were lost; however, STLs and 3D

901 PDFs of these elements are available (see here:

902 https://www.morphosource.org/Detail/MediaDetail/Show/media_id/33743) and all elements that

903 were individually scanned were also scanned with the full skull.

904

905 **Supporting information**

906 Additional Supporting Information can be found in the online version of this article:

907 **Appendix S1.** 3D PDF of segmented CT scans of the reassembled skull of *Protoichthyosaurus*

908 *prostaxalis* (BMT 1955.G35.1). Download the PDF file and click once on the skull to activate.

909 Left-click to rotate the model; right-click to zoom in or out; and hold both buttons to pan. Check

910 or uncheck boxes in the model tree in the upper left corner of the viewer to display or hide

911 individual parts.

912 **Appendix S2.** Transformation matrices for the 3D digital reconstruction of *Protoichthyosaurus*

913 *prostaxalis* (BMT 1955.G35.1) from original CT data.

914 **Appendix S3.** 3D PDF of the reconstructed skull of *Protoichthyosaurus prostaxalis* (BMT

915 1955.G35.1).

916

917 **References**

918 Andrew, CW. 1910. *A descriptive catalogue of the marine reptiles of the Oxford Clay. Part I.*

919 British Museum (Natural History), London, 205 pp.

920 Appleby RM. 1979. The affinities of Liassic and later ichthyosaurs. *Palaeontology* **22**:921–946.

921 Benton MJ, Spencer PS. 1995. Fossil Reptiles of Great Britain. Chapman and Hall, London, 386

922 pp.

923 Benton MJ, Taylor MA. 1984. Marine reptiles from the Upper Lias (Lower Toarcian, Lower

924 Jurassic) of the Yorkshire coast. *Proceedings of the Yorkshire Geological Society* **44**:399-429.

925 Bonaparte CL. 1841. A new systematic arrangement of vertebrated animals. *Transactions of the*

926 *Linnean Society of London* **18**:247-304.

927 Button D, Barrett P, Rayfield E. 2016. Comparative cranial myology and biomechanics of

928 *Plateosaurus* and *Camarasaurus* and evolution of the sauropod feeding apparatus.

929 *Palaeontology* **59**:887-913.

930 Cox P, Rinderknecht A, Blanco R. 2015. Predicting bite force and cranial biomechanics in the

931 largest fossil rodent using finite element analysis. *Journal of Anatomy* **226**:215-223.

932 Dal Sasso C, Maganuco S, Cioffi A. 2009. A neurovascular cavity within the snout of the

933 predatory dinosaur *Spinosaurus*. *First International Congress on North African Vertebrate*

934 *Palaeontology*, 22-23.

935 d'Orbigny A. 1842-1851. Paléontologie française. Terrains jurassiques. Tome I. Cephalopodes.

936 Masson, Paris, 642 pp.

937 De Blainville HD. 1835. Description de quelques espèces de reptile de la Californie, précédée de

938 l'analyse d'un système general d'Erpétologie et d'Amphibiologie. *Nouvelles*

939 *Annales du Muséum d'Histoire Naturelle* **4**:233-295.

940 Delair JB. 1969. A history of the early discoveries of Liassic ichthyosaurs in Dorset and

941 Somerset (1779–1835). *Proceedings of the Dorset Natural History and Archaeological Society*

942 **90**:1-9.

943 Edmonds EA, Poole EG, Wilson V. 1965. Geology of the country around Banbury and Edge

944 Hill: (explanation sheet 201, new series). HMSO.

945 Fernández M, Carabajal A, Gasparini Z, Diaz G. 2011. A metriorhynchid crocodyliform

946 braincase from northern Chile. *Journal of Vertebrate Paleontology* **31**:369–377.

947 Fischer V, Masure E, Arkhangelsky MS, Godefroit P. 2011. A New Barremian (Early

948 Cretaceous) ichthyosaur from western Russia. *Journal of Vertebrate Paleontology* **31**:1010-

949 1025.

950 Fischer V, Maisch MW, Naish D, Kosma R, Liston J. 2012. New ophthalmosaurid ichthyosaurs

951 from the European Lower Cretaceous demonstrate extensive ichthyosaur survival across the

952 Jurassic-Cretaceous boundary. *PLoS ONE* **7**:e29234.

953 Fischer V, Arkhangelsky MS, Uspensky GN, Stenshin IM. 2014. A new Lower Cretaceous

954 ichthyosaur from Russia reveals skull shape conservatism within Ophthalmosaurinae. *Geological*

955 *Magazine* **151**:60-70.

956 Fischer V, Bardet N, Benson BJ, Arkhangelsky MS, Friedman M. 2016. Extinction of fish-

957 shaped marine reptiles associated with reduced evolutionary rates and global environmental

958 volatility. *Nature Communications* **7**: 10825.

959 Foffa D, Cuff A, Sassoon J, Rayfield E, Mavrogordato M, Benton M. 2014a. Functional anatomy

960 and feeding biomechanics of a giant Upper Jurassic pliosaur (Reptilia: Sauropterygia) from

961 Weymouth Bay, Dorset, UK. *Journal of Anatomy* **225**:209-219.

962 Foffa D, Sassoon J, Cuff A, Mavrogordata M, Benton M. 2014b. Complex rostral neurovascular

963 system in a giant pliosaur. *Naturwissenschaften* **101**:453-456.

964 Herrera Y, Fernández M, Gaspirini Z. 2013. The snout of *Cricosaurus araucanensis:* a case

965 study in novel anatomy of the nasal region of metriorhynchids. *Lethaia* **46**:331-340.

966 Jasinoski S, Rayfield E, Chinsamy A. 2009. Comparative feeding biomechanics of *Lystrosaurus*

967 and the generalized dicynodont *Oudenodon. Anatomical Record* **292**:862-874.

968 Kear B. 2005. Cranial morphology of *Platypterygius longmani* Wade, 1990 (Reptilia:

969 Ichthyosauria) from the Lower Cretaceous of Australia. *Zoological Journal of the Linnean*

970 *Society* **145**:583-622.

971 Ketchum HF, Smith AS. 2010. The anatomy and taxonomy of *Macroplata tenuiceps*

972 (SAuropterygia, Plesiosauria) from the Hettangian (Lower Jurassic) of Warwickshire, United

973 Kingdom. *Journal of Vertebrate Paleontology* **30**:1066-1081.

974 Ketchum HF, Benson RBJ. 2011. The cranial anatomy and taxonomy of *Peloneustes philarchus*

975 (Sauropterygia, Pliosauridae) from the Peterborough Member (Callovian, Middle Jurassic) of the

976 United Kingdom. *Palaeontology* **54**:639-665.

977 Kirton AM. 1983. A review of British Upper Jurassic ichthyosaurs. Unpublished PhD thesis,

978 University of Newcastle upon-Tyne, 239 pp.

979 Larkin NR, Lomax DR, Meehitiya L, Dey S. 2016. The discovery in a museum collection of the

980 largest known skeleton of *Ichthyosaurus* in the world and its re-display, including 3D-printing

981   missing bones. *The Annual Symposium of Vertebrate Palaeontology and Comparative Anatomy.*

982   Vol 64, p. 12.

983   Larkin NR, O'Connor S, Parsons D. 2010. The virtual and physical preparation of the Collard

984   plesiosaur from Bridgwater Bay, Somerset, UK. *The Geological Curator* **9**:107-116.

985   Lautenschlager S. 2016. Reconstructing the past: methods and techniques for the digital

986   restoration of fossils. *Royal Society Open Science* **3**:doi: 10.1098/rsos.160342.

987   Lautenschlager S, Witmer L, Aaltangerel P, Zanno L, Rayfield E. 2014. Cranial anatomy of

988   *Erlikosaurus andrewsi* (Dinosauria, Therizinosauria): new insights based on digital

989   reconstruction. *Journal of Vertebrate Paleontology* **34**:1263-1291.

990   Lautenschlager S, Brassey C, Button D, Barrett P. 2016. Decoupled form and function in

991   disparate herbivorous dinosaur clades. *Scientific Reports* **6**:26495. doi: 10.1038/srep26495.

992   Lautenschlager S, Gill P, Luo Z, Fagan M, Rayfield E. 2017. Morphological evolution of the

993   mammalian jaw adductor complex. *Biological Reviews* **92**:1910-1940.

994   Lomax DR, Gibson BJA. 2015. The first definitive occurrence of *Ichthyosaurus* and

995   *Temnodontosaurus* (Reptilia: Ichthyosauria) in Nottinghamshire, England and a review of

996   ichthyosaur specimens from the county. *Proceedings of the Geologists' Association* **126**:554-

997   563.

998   Lomax DR, Massare JA. 2015. A new species of *Ichthyosaurus* from the Lower Jurassic of west

999   Dorset, England. *Journal of Vertebrate Paleontology* **35**:e903260.

1000   Lomax DR, Massare JA. 2017. Two new species of *Ichthyosaurus* from the lowermost Jurassic

1001   (Hettangian) of Somerset, England. *Papers in Palaeontology* **3**:1-20.

1002   Lomax DR, Massare JA. 2018. A second specimen of *Protoichthyosaurus applebyi* (Reptilia:

1003   Ichthyosauria) and additional information on the genus and species. *Paludicola* **11**:164-178.

1004 Lomax DR, Massare JA, Mistry R. 2017. The taxonomic utility of forefin morphology in Lower

1005 Jurassic ichthyosaurs: *Protoichthyosaurus* and *Ichthyosaurus*. *Journal of Vertebrate*

1006 *Paleontology* **37**:e1361433.

1007 Lomax DR, Sachs S. 2017. On the largest *Ichthyosaurus*: A new specimen of *Ichthyosaurus*

1008 *somersetensis* containing an embryo. *Acta Palaeontologica Polonica* **62**:575-584.

1009 Lomax DR, De La Salle P, Massare JA, Gallois R. 2018. A giant Late Triassic ichthyosaur from

1010 the UK and a reinterpretation of the Aust Cliff 'dinosaurian' bones. *PLOS ONE* **13**:e0194742.

1011 Maisch MW, Hungerbühler A. 1997. Revision of *Temnodontosaurus nuertingensis* (v. Huene,

1012 1931), a large ichthyosaur from the Lower Pliensbachian (Lower Jurassic) of Nurtingen, South

1013 Western Germany. *Stuttgarter Beiträge zur Naturkunde Serie B* **248**:1-11.

1014 Maisch MW. 2002. A braincase of *Temnodontosaurus* cf. *trigonodon* (von Theodori, 1843)

1015 (Ichthyosauria) from the Lower Jurassic of Germany. *Geologica et Palaeontololgica* **36**:115-122.

1016 Marek R, Moon B, Williams M, Benton M. 2015. The skull and endocranium of a Lower

1017 Jurassic ichthyosaur based on digital reconstructions. *Palaeontology* **58**:723-742.

1018 Martin JE, Frey E, Riess J. 1986. Soft-tissue preservation in ichthyosaurs and a stratigraphic

1019 review of the Lower Hettangian of Barrow-upon-Soar, Leicestershire. *Transactions of the*

1020 *Leicestershire Literary & Philosophical Society* **80**:58-72.

1021 Massare JA, Lomax DR. 2017. A taxonomic reassessment of *Ichthyosaurus communis* and *I.*

1022 *intermedius* and a revised diagnosis for the genus. *Journal of Systematic Palaeontology* **16**:263-

1023 277.

1024 McGowan C. 1973. The cranial morphology of the Lower Liassic latipinnate ichthyosaurs of

1025 England. *Bulletin of the British Museum (Natural History) Geology* **24**: 1-109.

1026 McGowan C. 1989. Computed tomography reveals further details of *Excalibosaurus,* a putative

1027 ancestor for the swordfish-like ichthyosaur *Eurhinosaurus. Journal of Vertebrate Paleontology*

1028 **9**:269-281.

1029 McGowan C. 1993. A new species of large, long-snouted ichthyosaur from the English lower

1030 Lias. *Canadian Journal of Earth Sciences* **30**:1197-1204.

1031 McGowan C. 1996a. The taxonomic status of *Leptopterygius* Huene, 1922 (Reptilia:

1032 Ichthyosauria). *Canadian Journal of Earth Sciences* **33**:439-443.

1033 McGowan C. 1996b. Giant ichthyosaurs of the Early Jurassic. *Canadian Journal of Earth*

1034 *Sciences* **33**:1011-1021.

1035 McGowan C. 2003. A new specimen of *Excalibosaurus* from the English Lower Jurassic.

1036 *Journal of Vertebrate Paleontology* **23**:950-956.

1037 McGowan C, Motani R. 2003. Handbook of Paleoherpetology, Part 8 Ichthyopterygia. Verlag

1038 Dr. Friedrich Pfeil pp. 175.

1039 Milner AC, Walsh S. 2010. Reptiles. In: Lord, A.R., Davis, P.G. (Eds.), Fossils from the Lower

1040 Lias of the Dorset Coast. The Palaeontological Association, pp. 372–394.

1041 Moon BC, Kirton AM. 2016. Ichthyosaurs of the British Middle and Upper Jurassic. Part 1 -

1042 *Ophthalmosaurus. Monograph of the Palaeontographical Society* **170**:1-84.

1043 Motani R. 1999. On the evolution and homologies of ichthyopterygian forefins. *Journal of*

1044 *Vertebrate Paleontology* **19**:28-41.

1045 Motani R. 2005. Evolution of fish-shaped reptiles (Reptilia: Ichthyopterygia) in their physical

1046 environments and constraints. *Annual Review of Earth and Planetary Sciences*, **33**:395-420.

1047 Motani R. 2009. The evolution of marine reptiles. *Evolution: Education and Outreach* **2**:224-

1048 235.

1049   Neenan J, Scheyer T. 2012. The braincase and inner ear of *Placodus gigas* (Sauropterygia,

1050   Placodontia) – a new reconstruction based on micro-computed tomographic data. *Journal of*

1051   *Vertebrate Paleontology* **32**:1350-1357.

1052   Nicholls EL, Manabe M. 2004. Giant ichthyosaurs of the Triassic—A new species of

1053   *Shonisaurus* from the Pardonet Formation (Norian: Late Triassic) of British Columbia. *Journal*

1054   *of Vertebrate Paleontology* **24**:838–849.

1055   Porro L, Rayfield, E, Clack J. 2015a. Descriptive anatomy and three-dimensional reconstruction

1056   of the skull of the early tetrapod *Acanthostega gunnari* Jarvik, 1952. *PLOS ONE* **10**:e0118882.

1057   doi: 10.1371/journal.pone.0118882.

1058   Porro L, Rayfield E, Clack J. 2015b. Computed tomography, anatomical description and three-

1059   dimensional reconstruction of the lower jaw of *Eusthenopteron foordi* Whiteaves, 1881 from the

1060   Upper Devonian of Canada. *Palaeontology* **58**:1031-1047.

1061   Porro L, Witmer L, Barrett P. 2015c. Digital preparation and osteology of the skull of

1062   *Lesothosaurus diagnosticus* (Ornithischia: Dinosauria). *PeerJ* **3**:e1494. doi: 10.7717/peerj.1494.

1063   Quenstedt FA. 1858. Der Jura. Tübingen pp. 842.

1064   Radley JD. 2003. Warwickshire's Jurassic geology: past, present and future. *Mercian Geologist*

1065   **15**:209-218.

1066   Rayfield E, Norman D, Horner C, Horner J, Smith P, Thomason J, Upchurch P. 2001. Cranial

1067   design and function in a large theropod dinosaur. *Nature* **409**:1033-1037.

1068   Sato T, Wu X, Tirabasso A, Bloskie P. 2011. Braincase of a polycotylid plesiosaur (Reptilia:

1069   Sauropterygia) from the Upper Cretaceous of Manitoba, Canada. *Journal of Vertebrate*

1070   *Paleontology* **31**:313–329.

1071 Seeley HG. 1874. On the pectoral arch and forelimb of *Ophthalmosaurus*, a new ichthyosaurian

1072 genus from the Oxford Clay. Qu*arterly Journal of the Geological Society of London* **30**:696-707.

1073 Sharp A. 2014. Three dimensional digital reconstruction of the jaw adductor musculature of the

1074 extinct marsupial giant *Diprotodon optatum*. *PeerJ* **2**:e514. doi: 10.7717/peerj.514.

1075 Smith AS, Radley JD. 2007. A marine reptile fauna from the Early Jurassic Saltford Shale (Blue

1076 Lias Formation) of central England. *Proceedings of the Yorkshire Geological Society* **56**:253-

1077 260.

1078 Sollas WJ. 1916. The skull of *Ichthyosaurus,* studied in serial sections. *Philosophical*

1079 *Transactions of the Royal Society of London, Series B* **208**:63-126.

1080 VanBuren CS, Evans DC. 2017. Evolution and function of anterior cervical vertebral fusion in

1081 tetrapods. *Biological Reviews* **92**:608-626.

1082 Wade M. 1990. A review of the Australian Cretaceous longipinnate ichthyosaur *Platypterygius*

1083 (Ichthyosauria: Ichthyopterygia). *Memoirs of the Queensland Museum* **28**: 115-137

1084 Williams M, Benton MJ, Ross A. 2015. The Strawberry Bank Lagerstätte reveals insights into

1085 Early Jurassic life. *Journal of the Geological Society* **172**:683-692.

1086 Witmer LM. 1997. The evolution of the antorbital cavity of archosaurs: a study in soft-tissue

1087 reconstruction in the fossil record with an analysis of the function of pneumaticity. *Society of*

1088 *Vertebrate Paleontology Memoir* **3**:1-73.

1089 Wroe S. 2007. Cranial mechanics compared in extinct marsupial and extant African lions using a

1090 finite-element approach. *Journal of Zoology* **4**:332-339.

1091 Young M, Bird J. 1828. A geological survey of the Yorkshire Coast: describing the strata and

1092 fossils occurring between the Humber and the Tees, from the German ocean to the plain of York.

1093 Whitby 368 pp.

1094

1095   **Figures**

1096

1097   **Figure 1.** Three-dimensional skull of BMT 1955.G35.1, *Protoichthyosaurus prostaxalis*. A,

1098   original photograph of the first skull reconstruction (left lateral view) within a couple of years of

1099   the 1955 excavation. Note that the prefrontal and postorbital are present, which we have been

1100   unable to locate in our study. B, skull in left lateral view, as reconstructed in 2015. C, skull in

1101   right lateral view, as reconstructed in 2015. Note the distinctive asymmetric maxilla with long,

1102   narrow anterior process. Teeth are not in their original positions. Scale bar represents 20 cm.

1103

1104   **Figure 2.** Surface models (generated from CT scan data) of preserved bones from the upper jaw

1105   of BMT 1955.G35.1, *Protoichthyosaurus prostaxalis*. Right (A) and left (B) lateral views of the

1106   cranium. Medial views of the right (C) and left (D) sides of the cranium. Dorsal (E) and ventral

1107   (F) views of the cranium. Lateral views of the right (G) and left (H) premaxillae. Dorsal views of

1108   the right (I) and left (J) premaxillae. Posterior (K) view of the upper jaw. Individual bones are

1109   shown in different colors. Bones in G–J are transparent to visualize internal canals (shown in red

1110   opaque). Teeth are not in their original positions. *Abbreviations*: bs, basioccipital; ex,

1111   exoccipital; f?, possible fragment of frontal; j, jugal; l, lacrimal; mx, maxilla; n, nasal; p, parietal;

1112   pf, prefrontal; pmx, premaxilla; pt, pterygoid; q, quadrate; so, supraoccipital; sp, supratemporal;

1113   st, stapes. Scale bars equal 10 cm.

1114

1115   **Figure 3.** Surface models (generated from micro-CT scan data) of preserved palatal and

1116   braincase bones from BMT 1955.G35.1, *Protoichthyosaurus prostaxalis*. Right medial (A) and

1117   left lateral (B) views, dorsal (C) and ventral (D) views, and anterior (E) and posterior (F) views.

1118   Isolated supraoccipital in right anterolateral view (G). Individual bones are shown in different

1119   colors. Supraoccipital in G is transparent to visualize internal canals (shown in red opaque).

1120   *Abbreviations*: bs, basioccipital; ex, exoccipital; f?, probable fragment of upper pterygoid wing;

1121   p, parietal; pt, pterygoid; q, quadrate; se, sella turcica; so, supraoccipital; sp, supratemporal; st,

1122   stapes. Scale bars equal 10 cm, except for (G) which equals 5 cm.

1123

1124   **Figure 4.** Surface models (generated from CT scan data) of preserved bones from the lower jaw

1125   of BMT 1955.G35.1, *Protoichthyosaurus prostaxalis*. Lateral views of the right (A) and left (B)

1126   lower jaws. Medial views of the right (C) and left (D) lower jaws. Dorsal (E) and ventral (F)

1127   views of the both halves of the lower jaws. Lateral views of the right (G) and left (H) dentary.

1128   Ventral views of the right (I) and left (J) dentaries. Lateral oblique (K) view of the left

1129   surangular. Individual bones are shown in different colors. Bones in G–K are transparent to

1130   visualize internal canals (shown in red opaque). Teeth are not in their original positions.

1131   *Abbreviations*: an, angular; ar, articular, d, dentary; f?, possible surangular fragment; sa,

1132   surangular; sp, splenial; spf, splenial fragment. Scale bars equal 10 cm.

1133

1134   **Figure 5.** Elements of the skull, palate, lower jaw and dentition of BMT 1955.G35.1,

1135   *Protoichthyosaurus prostaxalis*. A-D, incomplete and damaged, articulated parietals in dorsal

1136   (A), ventral (B), posterior (C) and anterior (D) view. E-F, incomplete and damaged left pterygoid

1137   in posterior (E) and ventral (F) view. Note the three wing-like projections in posterior view. G-I,

1138   incomplete and damaged left quadrate in anterior (G), posterior (H) and lateral (I) view. J, hyoids

1139   in dorsal view. K-L, incomplete and damaged right nasal in dorsal (K) and (L) lateral view. M,

1140 incomplete and damaged right postfrontal in dorsal view. N, practically complete tooth missing

1141 the tip of the crown. Note that the root is large with prominent grooves that extend to the base of

1142 the crown and continue as longitudinal striations on the crown. *Abbreviations*: ac, articular

1143 condyle; (?)ce, impression of cerebellum; ch, impression of cerebral hemisphere; dpf, descending

1144 parietal flange; eed, extra-encephalic depression; ocl, occipital lamella; ol, impression of optic

1145 lobe; op, elongate openings in the posterior surface of the parietal; par, palatal ramus; ps, parietal

1146 shelf (ridge); qf, quadratojugal facet; sc, sagittal crest; spt, supratemporal probably fused with

1147 parietals; vs, ventral surface. Scale bars represent 3 cm.

1148

1149 **Figure 6.** Braincase elements of BMT 1955.G35.1, *Protoichthyosaurus prostaxalis*. A-C,

1150 incomplete supraoccipital in posterior (A), dorsal (B) and ventral (C) view. D-E,

1151 parabasisphenoid with complete basisphenoid and broken parasphenoid in anterior (D) and

1152 ventral (E) view. F-G, left opisthotic in anteromedial (F) and ventrolateral (G) view. Note the 'V-

1153 shaped' membranous impression in F. H, incomplete left stapes in posterior view. *Abbreviations*:

1154 bf, facet for basipterygoid facet; bof, basioccipital facet; bp, basipterygoid process; cf, carotid

1155 foramen; ds, dorsum sellae; ef, exoccipital facet; hsc, horizontal semicircular canal; (?)ma,

1156 muscle attachment; mh, medial head; mr, median ridge; p, base of parasphenoid; pp, paroccipital

1157 process; pvsc, posterior vertical semicircular canal; rfm, roof of foramen magnum; sac, sacculus;

1158 sf, stapedial facet; st, sella turcica; t, paired trabeculae; tg, trenchant groove; (?)ut, utriculus.

1159 Scale bars represent 3 cm.

1160

1161 **Figure 7.** Elements of the postcranial skeleton of BMT 1955.G35.1, *Protoichthyosaurus*

1162 *prostaxalis*. A-B, probable 'unfused' (see text for details) axis vertebra in anterior (A) and

1163   ventral (B) view. Note the unusual, almost rugose anterior surface. The dark, circular element to

1164   the right is a poorly preserved bivalve mollusk. C, left coracoid in dorsal view. D, incomplete left

1165   scapula in lateral view. E-F, left humerus in dorsal (E) and ventral (F) view. Note that the dorsal

1166   process (trochanter dorsalis) is damaged, as is the facet for the ulna. G, complete ilium in either

1167   lateral or medial view. Note that the posterior end (to the right) is bulbous, relative to the shaft.

1168   H-I, damaged (?)right femur in dorsal (H) and ventral (view). *Abbreviations*: af, anterior facet;

1169   aif, facet for the axial intercentrum; an, anterior notch; bpe, broken posterior end; bpe, bulbous

1170   posterior end; ccf, facet for the cervical centrum; dp, dorsal process; dpc, deltopectoral crest; ff,

1171   fibular facet; gf, glenoid facet; if, intercoracoid facet; pm?, predation marks; pn, posterior notch;

1172   rf, radial facet; sf, scapular facet; tf, tibial facet; uf, ulnar facet; vp, ventral process. Scale bars

1173   represent 3 cm.

1174

1175   **Figure 8.** Surface models (generated from CT scan data) of the reassembled skull of BMT

1176   1955.G35.1, *Protoichthyosaurus prostaxalis,* highlighting differences between fossil bone

1177   (grey), regions reconstructed during original reassembly in the 1950s (yellow), and regions

1178   reconstructed in the course of the current work (blue). Right (A) and left (B) lateral, and dorsal

1179   (C) and ventral (D) views of the upper and lower jaws.

1180

1181   **Figure 9.** Surface models (generated from CT scan data) of the skull of BMT 1955.G35.1,

1182   *Protoichthyosaurus prostaxalis,* after the removal of minor damage and duplication/mirroring of

1183   asymmetrically preserved elements, and digital articulation of individual bones to produce a

1184   more accurate digital 3D reconstruction. Displacement of the lower jaw and premaxillae and

1185   nasals are the result of deformation (see text). Left lateral (A), dorsal (B), ventral (C), anterior

1186   (D), and posterior (E) views of the upper and lower jaws. Individual bones labelled using the

1187   same colors as Figures 2–4.

1188

Figure 1

Three-dimensional skull of BMT 1955.G35.1, *Protoichthyosaurus prostaxalis*.

A, original photograph of the first skull reconstruction (left lateral view) within a couple of years of the 1955 excavation. Note that the prefrontal and postorbital are present, which we have been unable to locate in our study. B, skull in left lateral view, as reconstructed in 2015. C, skull in right lateral view, as reconstructed in 2015. Note the distinctive asymmetric maxilla with long, narrow anterior process. Teeth are not in their original positions. Scale bar represents 20 cm.
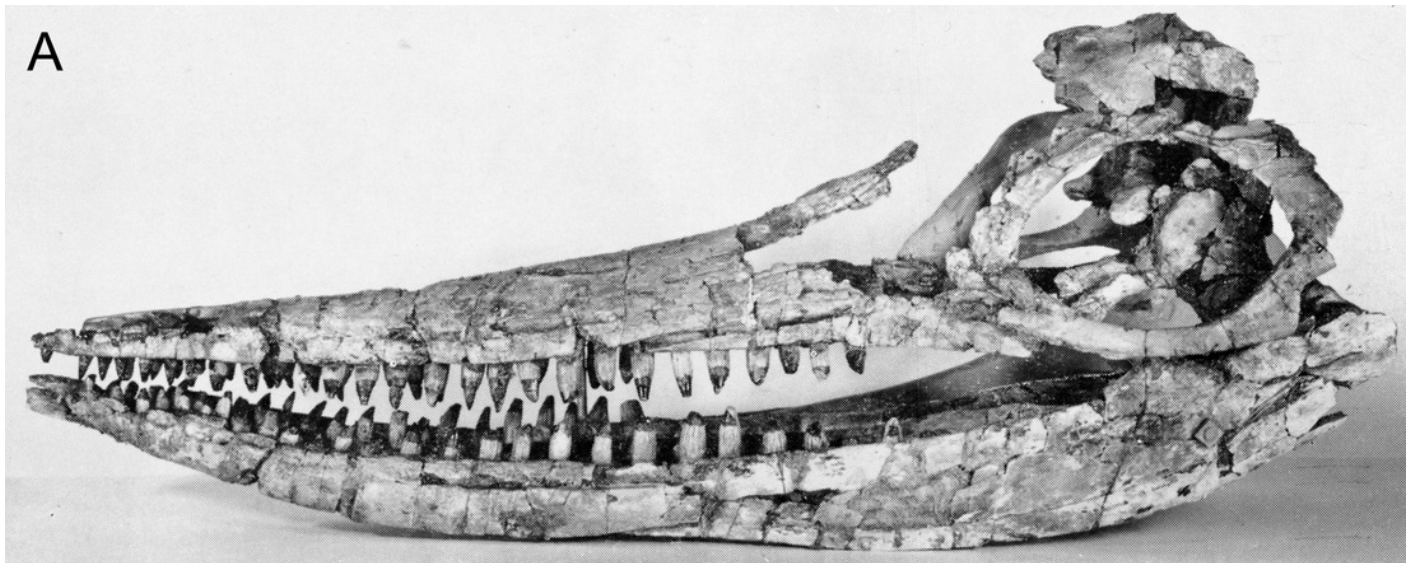
Figure 2

Surface models (generated from CT scan data) of preserved bones from the upper jaw of BMT 1955.G35.1, *Protoichthyosaurus prostaxalis*.

Right (A) and left (B) lateral views of the cranium. Medial views of the right (C) and left (D) sides of the cranium. Dorsal (E) and ventral (F) views of the cranium. Lateral views of the right (G) and left (H) premaxillae. Dorsal views of the right (I) and left (J) premaxillae. Posterior (K) view of the upper jaw. Individual bones are shown in different colors. Bones in G–J are transparent to visualize internal canals (shown in red opaque). Teeth are not in their original positions. *Abbreviations*: bs, basioccipital; ex, exoccipital; f?, possible fragment of frontal; j, jugal; l, lacrimal; mx, maxilla; n, nasal; p, parietal; pf, prefrontal; pmx, premaxilla; pt, pterygoid; q, quadrate; so, supraoccipital; sp, supratemporal; st, stapes. Scale bars equal 10 cm.
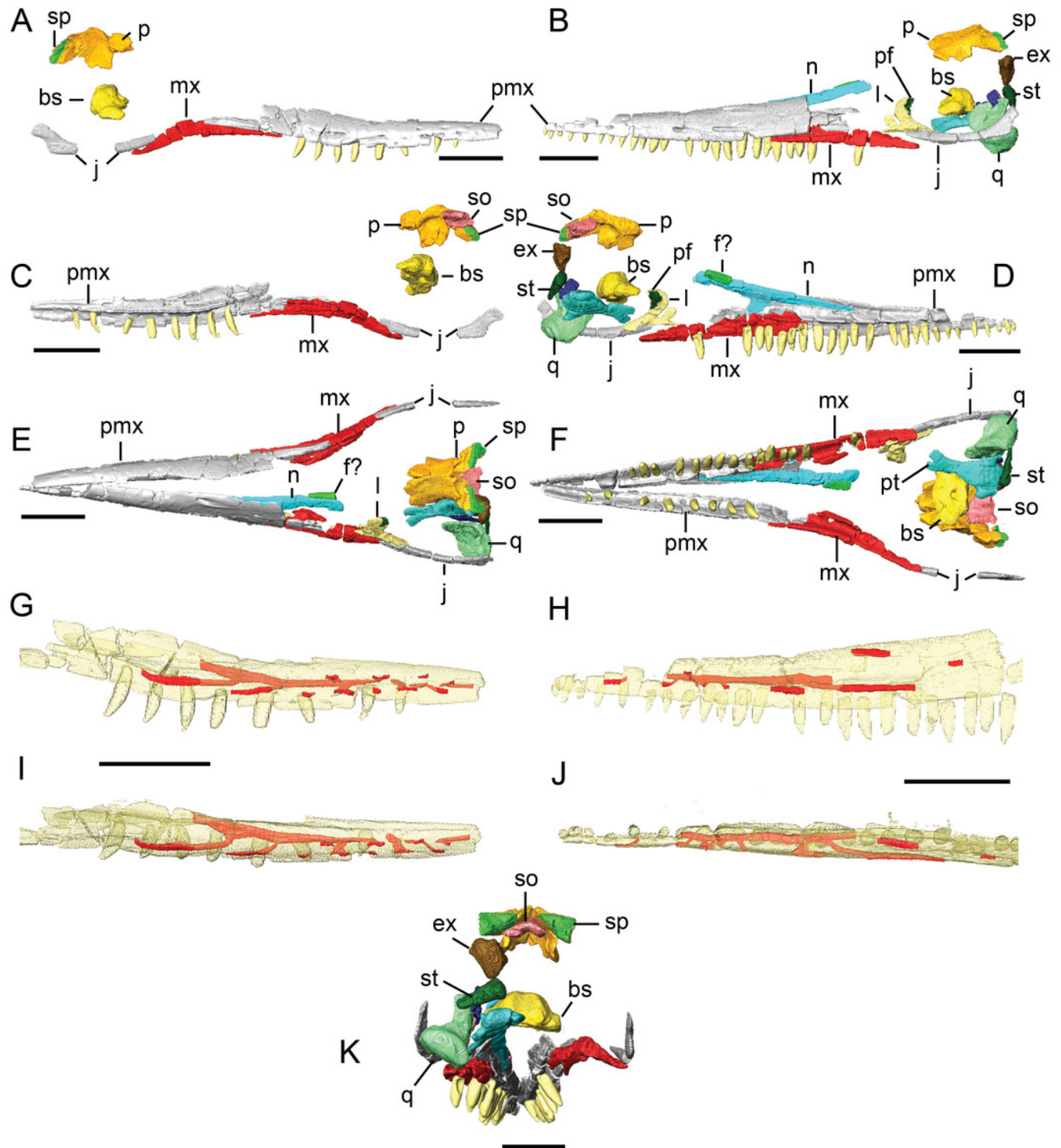
Figure 3

Surface models (generated from micro-CT scan data) of preserved palatal and braincase bones from BMT 1955.G35.1, *Protoichthyosaurus prostaxalis*.

Right medial (A) and left lateral (B) views, dorsal (C) and ventral (D) views, and anterior (E) and posterior (F) views. Isolated supraoccipital in right anterolateral view (G). Individual bones are shown in different colours. Supraoccipital in G is transparent to visualize internal canals (shown in red opaque). *Abbreviations*: bs, basioccipital; ex, exoccipital; f?, probable fragment of upper pterygoid wing; p, parietal; pt, pterygoid; q, quadrate; se, sella turcica; so, supraoccipital; sp, supratemporal; st, stapes. Scale bars equal 10 cm, except for (G) which equals 5 cm.
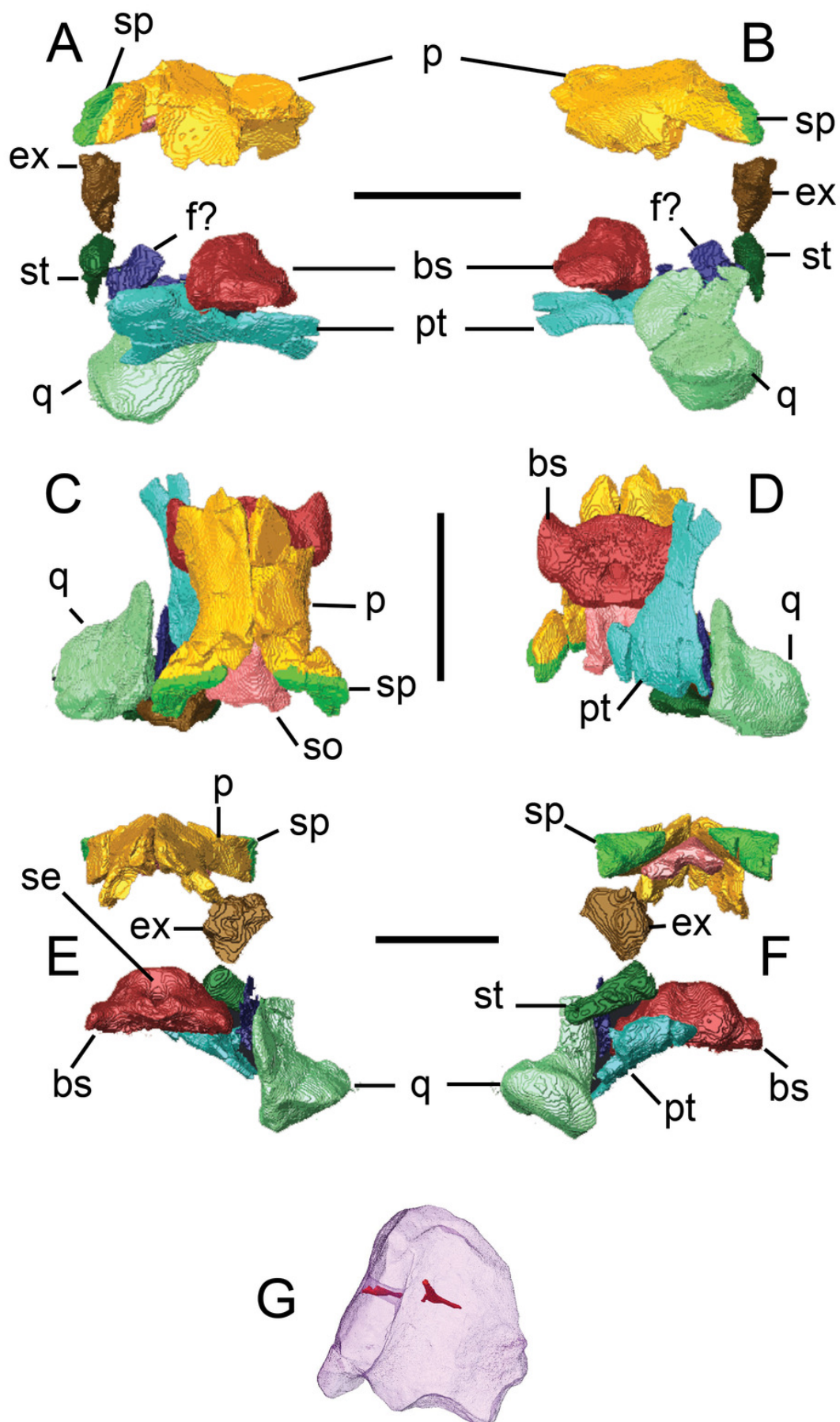
Figure 4

Surface models (generated from CT scan data) of preserved bones from the lower jaw of BMT 1955.G35.1, *Protoichthyosaurus prostaxalis*.

Lateral views of the right (A) and left (B) lower jaws. Medial views of the right (C) and left (D) lower jaws. Dorsal (E) and ventral (F) views of the both halves of the lower jaws. Lateral views of the right (G) and left (H) dentary. Ventral views of the right (I) and left (J) dentaries. Lateral oblique (K) view of the left surangular. Individual bones are shown in different colors. Bones in G–K are transparent to visualize internal canals (shown in red opaque). Teeth are not in their original positions. *Abbreviations*: an, angular; ar, articular, d, dentary; f?, possible surangular fragment; sa, surangular; sp, splenial; spf, splenial fragment. Scale bars equal 10 cm.
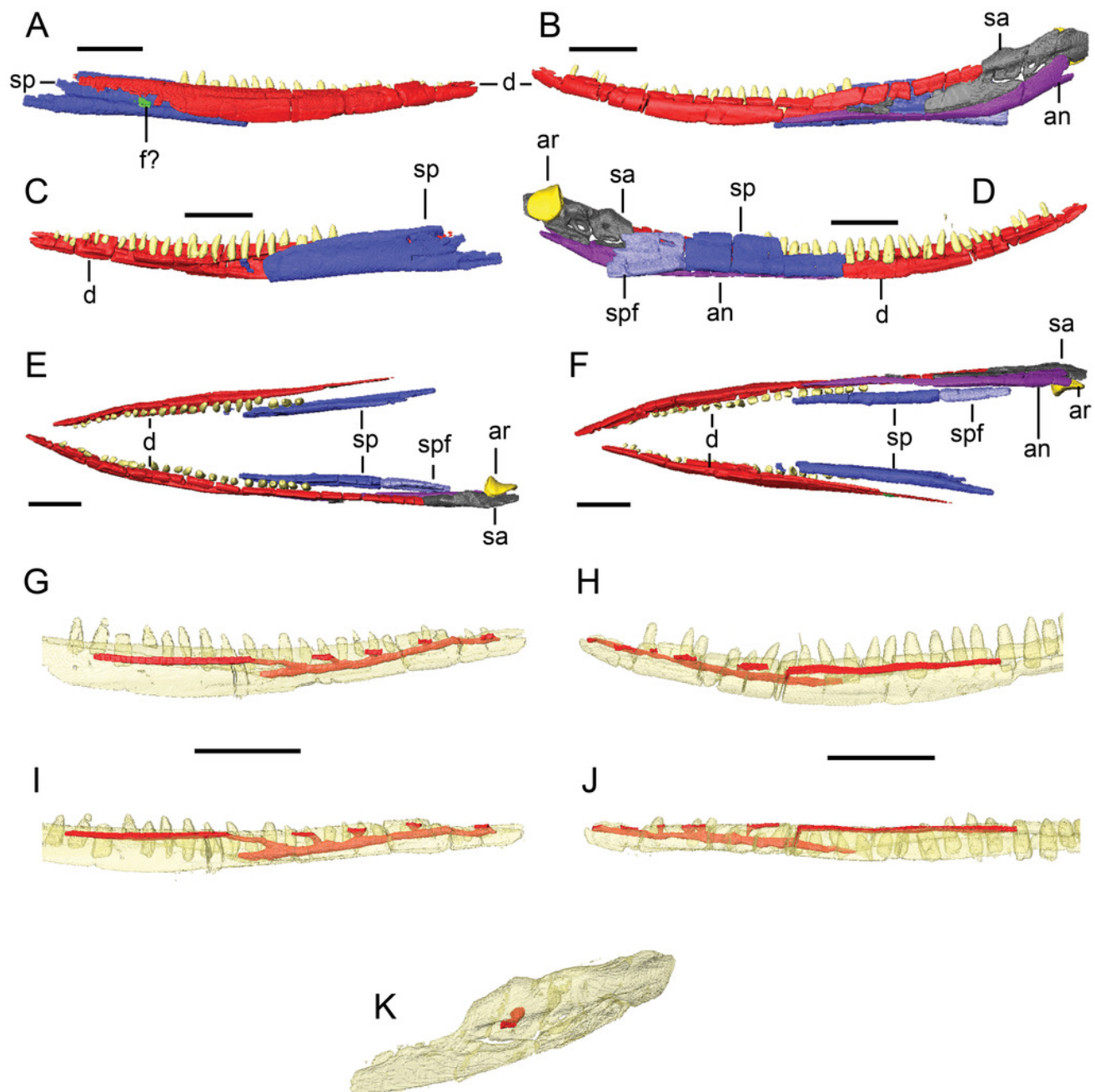
Figure 5

Elements of the skull, palate, lower jaw and dentition of BMT 1955.G35.1, *Protoichthyosaurus prostaxalis*.

A-D, incomplete and damaged, articulated parietals in dorsal (A), ventral (B), posterior (C) and anterior (D) view. E-F, incomplete and damaged left pterygoid in posterior (E) and ventral (F) view. Note the three wing-like projections in posterior view. G-I, incomplete and damaged left quadrate in anterior (G), posterior (H) and lateral (I) view. J, hyoids in dorsal view. K-L, incomplete and damaged right nasal in dorsal (K) and (L) lateral view. M, incomplete and damaged right postfrontal in dorsal view. N, practically complete tooth missing the tip of the crown. Note that the root is large with prominent grooves that extend to the base of the crown and continue as longitudinal striations on the crown. *Abbreviations*: ac, articular condyle; (?)ce, impression of cerebellum; ch, impression of cerebral hemisphere; dpf, descending parietal flange; eed, extra-encephalic depression; ocl, occipital lamella; ol, impression of optic lobe; op, elongate openings in the posterior surface of the parietal; par, palatal ramus; ps, parietal shelf (ridge); qf, quadratojugal facet; sc, sagittal crest; spt, supratemporal probably fused with parietals; vs, ventral surface. Scale bars represent 3 cm.
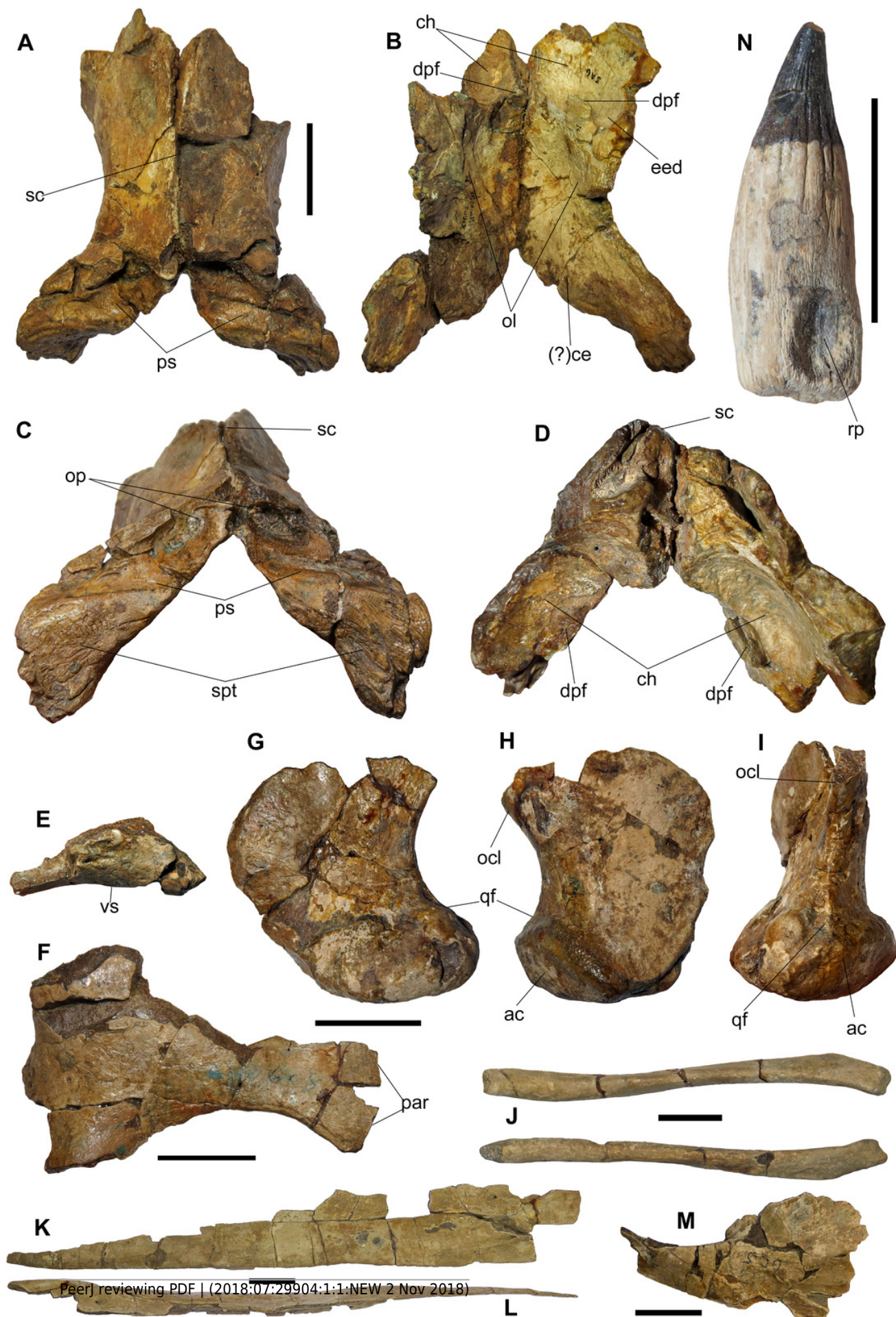
Figure 6

Braincase elements of BMT 1955.G35.1, *Protoichthyosaurus prostaxalis*.

A-C, incomplete supraoccipital in posterior (A), dorsal (B) and ventral (C) view. D-E, parabasisphenoid with complete basisphenoid and broken parasphenoid in anterior (D) and ventral (E) view. F-G, left opisthotic in anteromedial (F) and ventrolateral (G) view. Note the 'V-shaped' membranous impression in F. H, incomplete left stapes in posterior view. *Abbreviations*: bf, facet for basipterygoid facet; bof, basioccipital facet; bp, basipterygoid process; cf, carotid foramen; ds, dorsum sellae; ef, exoccipital facet; hsc, horizontal semicircular canal; (?)ma, muscle attachment; mh, medial head; mr, median ridge; p, base of parasphenoid; pp, paroccipital process; pvsc, posterior vertical semicircular canal; rfm, roof of foramen magnum; sac, sacculus; sf, stapedial facet; st, sella turcica; t, paired trabeculae; tg, trenchant groove; (?)ut, utriculus. Scale bars represent 3 cm.
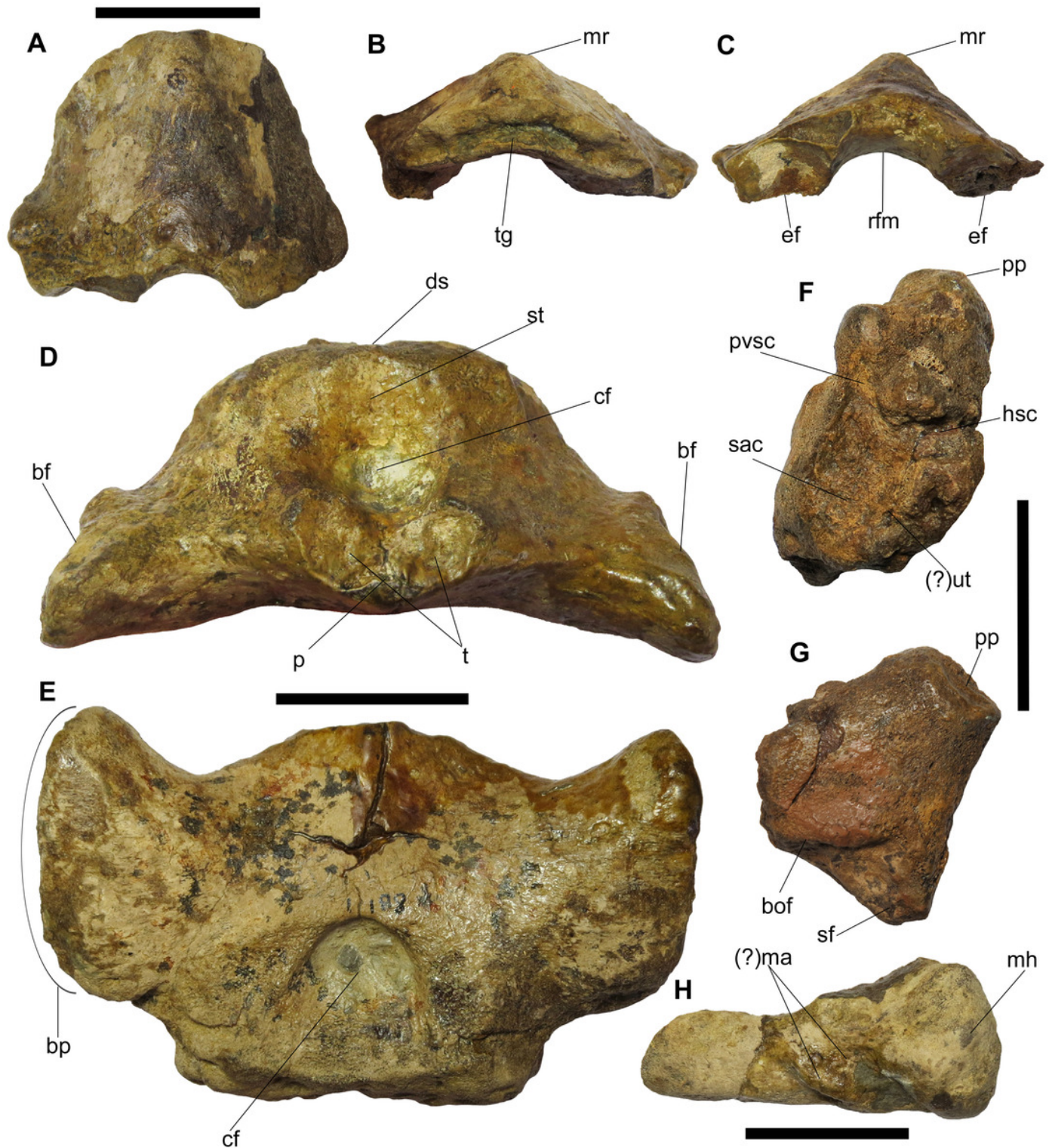
A

B   mr

tg

C   mr

ef   rfm   ef

D   ds   st   cf

bf   bf

p   t

E   pp

F   pvsc   hsc

sac   (?)ut

G   pp

bof   sf

bp   (?)ma   mh

cf   H

Figure 7

Elements of the postcranial skeleton of BMT 1955.G35.1, *Protoichthyosaurus prostaxalis*.

A-B, probable 'unfused' (see text for details) axis vertebra in anterior (A) and ventral (B) view. Note the unusual, almost rugose anterior surface rarely seen in ichthyosaurs. The dark, circular element to the right is a poorly preserved bivalve mollusc. C, left coracoid in dorsal view. D, incomplete left scapula in lateral view. E-F, left humerus in dorsal (E) and ventral (F) view. Note that the dorsal process (trochanter dorsalis) is damaged, as is the facet for the ulna. G, complete ilium in either lateral or medial view. Note that the posterior end (to the right) is bulbous, relative to the shaft. H-I, damaged (?)right femur in dorsal (H) and ventral (view). *Abbreviations*: af, anterior facet; aif, facet for the axial intercentrum; an, anterior notch; bpe, broken posterior end; bpe, bulbous posterior end; ccf, facet for the cervical centrum; dp, dorsal process; dpc, deltopectoral crest; ff, fibular facet; gf, glenoid facet; if, intercoracoid facet; pm?, predation marks; pn, posterior notch; rf, radial facet; sf, scapular facet; tf, tibial facet; uf, ulnar facet; vp, ventral process. Scale bars represent 3 cm.

Figure 8

Surface models (generated from CT scan data) of the skull of BMT 1955.G35.1, *Protoichthyosaurus prostaxalis,* highlighting differences between the original skull and reconstruction.

Fossil bone (grey), regions reconstructed during original reassembly in the 1950s (yellow), and regions reconstructed in the course of the current work (blue). Right (A) and left (B) lateral, and dorsal (C) and ventral (D) views of the upper and lower jaws.
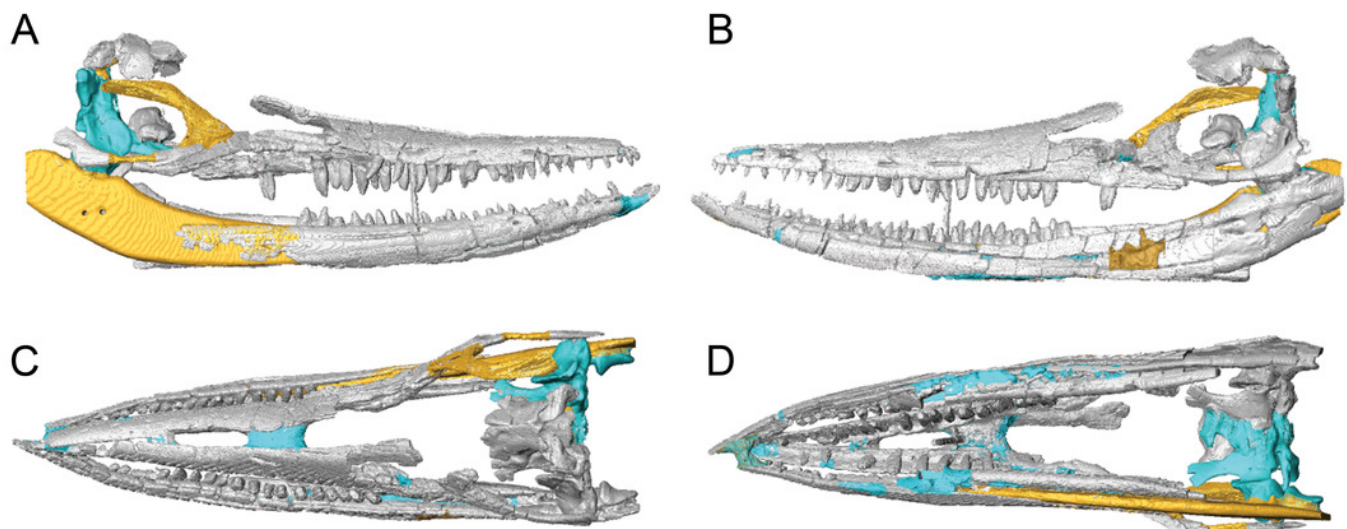
Figure 9

Surface models (generated from CT scan data) of the skull of BMT 1955.G35.1, *Protoichthyosaurus prostaxalis*.

After the removal of minor damage and duplication/mirroring of asymmetrically preserved elements, and digital articulation of individual bones to produce a more accurate digital 3D reconstruction. Displacement of the lower jaw and premaxillae and nasals are the result of deformation (see text). Left lateral (A), dorsal (B), ventral (C), anterior (D), and posterior (E) views of the upper and lower jaws. Individual bones labeled using the same colors as Figures 2–4.
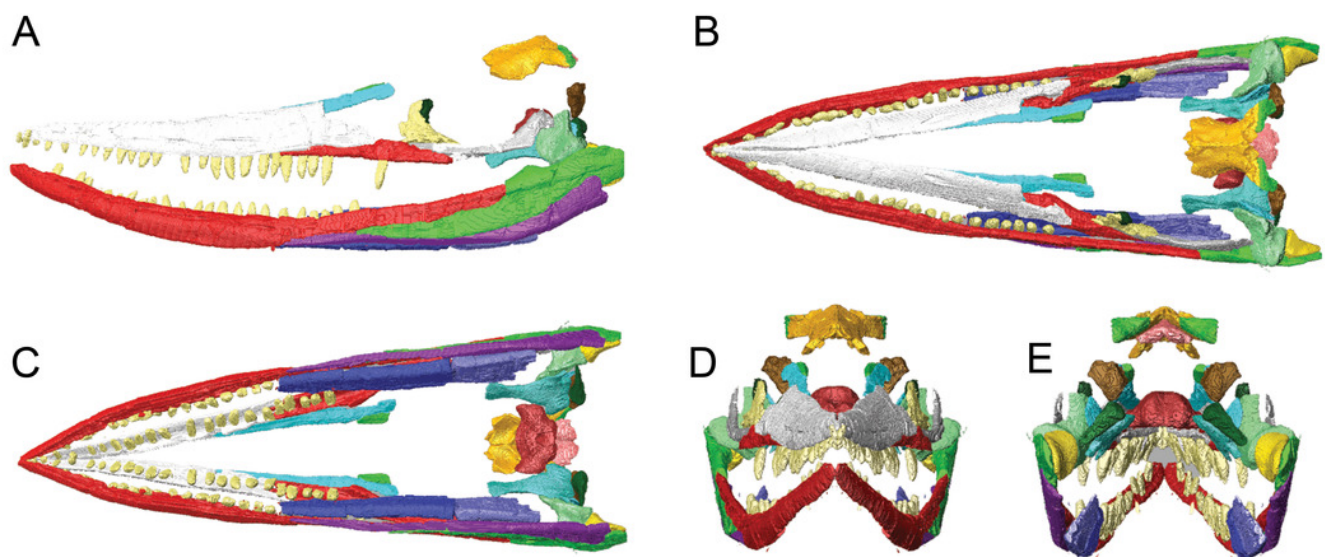
Measurements of some skull and postcranial elements of BMT 1955.G35.1,
Protoichthyosaurus prostaxalis.

'Width' for fin elements refers to the anteroposterior dimension, perpendicular to the long
axis of the fin. L and R denote measurement of left or right elements. Asterisk denotes an
estimate because the bone is damaged or elements are missing.

1   **Table 1**

2   Measurements of some skull and postcranial elements of BMT 1955.G35.1, *Protoichthyosaurus*

3   *prostaxalis*. 'Width' for fin elements refers to the anteroposterior dimension, perpendicular to the

4   long axis of the fin. L and R denote measurement of left or right elements. Asterisk denotes an

5   estimate because the bone is damaged or elements are missing.

Element	(cm)
Skull length	80*
Maxilla length	25.5R 24.2L*
Lower jaw length	87*
Basisphenoid length	5.82
Basisphenoid width	9.95
Supraoccipital height	5.04
Supraoccipital width	6.11
Quadrate length	9.4
Quadrate max width	8.2
Hyoid length	18.5R 18.2L
Coracoid med-lat length	12.16
Coracoid ant-post	13.66
Scapula preserved length	12.9*
Scapula proximal end only	7.25
Humerus length	10.4
Humerus distal width	8.59*
Humerus proximal width	7.66
Femur length	8.7
Femur distal width	5.1
Femur proximal width	2.5*
Ilium length	9.38
Humerus/Femur ratio	1.2